Politecnico di Torino

Politecnico di Torino

Energy and nuclear engineering

Academic Year 2024/2025

Graduation session November/December 2025

Development and Characterization of Multicomponent Thin Films on Silicon Substrates for Nuclear Applications

Advisor:

Prof. Monica Ferraris

Candidate:

Lorenzo Aldo Macario

Abstract

The growing demand for materials capable of withstanding extreme environments in advanced nuclear systems has led to increasing interest in alloys and coatings with enhanced mechanical strength and radiation tolerance. This thesis focuses on the development and preliminary characterization of multicomponent materials, specifically high-entropy alloys (HEAs), deposited as thin films on silicon substrates for practical and experimental reasons but ultimately intended for both coating and bulk applications in the nuclear field. The research combines theoretical analysis and experimental investigations conducted at the University of Tokyo in collaboration with the Murakami Group.

A comprehensive study of thin-film deposition technologies and material characterization techniques was first carried out to provide the scientific foundation for the experimental work. The deposited films were examined using optical microscopy and scanning electron microscopy to assess their morphology, surface roughness, and structural uniformity. Nanoindentation tests were also performed to collect preliminary data on the mechanical response of the films, including hardness and elastic modulus.

A central objective of this research was to test and evaluate the performance of the new PVD deposition system designed by Prof. Murakami, with particular attention to its efficiency, reproducibility, and data acquisition speed. The experimental results mainly consist of a systematic collection of morphological and mechanical data, which will serve as a foundation for future studies and for the identification of innovative, radiation-resistant materials suitable for next-generation nuclear systems.

Table of Contents

I. Introduction

i.1 Background and Motivation

The nuclear industry represents one of the most advanced and critical sectors of modern technology, with applications ranging from energy production to the medical field and advanced scientific research. One of the key aspects for the proper functioning and safety of nuclear facilities is the selection and development of materials capable of withstanding the extreme conditions to which they are subjected. Neutron and ion irradiation, high temperatures, and chemically aggressive environments impose extremely stringent requirements on the materials used in reactor structures and components. For this reason, research and innovation in the field of nuclear materials are essential not only to ensure the reliability and safety of facilities but also to improve their economic and operational efficiency. Enhancing material performance allows for reduced maintenance costs, increased component lifetimes, and minimized risk of unexpected failures, with clear benefits in terms of safety and economic sustainability.

This thesis is part of a broader research effort focused on the development of advanced materials for nuclear applications, with particular emphasis on multicomponent systems based on high-entropy alloys (HEAs). These materials are investigated not only as protective coatings but also as potential bulk materials for structural components exposed to extreme environments. The motivation behind this study arises from the need to enhance the resistance of materials used in nuclear facilities against radiation damage and wear caused by severe operating conditions. Neutron and ion irradiation [1][2] can significantly modify the mechanical and structural properties of materials, leading to degradation of their performance over time. The development of innovative multicomponent alloys, both in the form of thin films and bulk materials, aims to improve radiation tolerance, mechanical stability, and overall durability, thereby extending the operational lifetime of components and reducing maintenance and replacement costs. The selection and optimization of these advanced materials are therefore crucial, as their performance depends not only on their ability to withstand radiation but also on their chemical, thermal, and microstructural stability under extreme conditions.

The experimental work supporting this research was conducted at the laboratories of the University of Tokyo, in collaboration with Professor Murakami and his research team, known as the "Murakami Group." This collaboration enabled access to cutting-edge equipment and highly specialized know-how in the field of materials science applied to nuclear energy. The project took place over a five-month period, during which

extensive analysis was carried out on the properties and chemical/structural stability of the materials, all in relation to the deposition environments in which they were synthesized. Advanced characterization tools were employed, including Scanning Electron Microscopy (SEM) and optical microscopy, to investigate the surface and internal morphology of the materials. Mechanical properties were evaluated using a nanoindentation machine. Film deposition was carried out using a PVD system designed by Professor Murakami and custom-built by Seinan Kogyo Co., Ltd. [3] upon his commission. The choice of deposition techniques was carefully considered to identify the most effective method for achieving uniform and durable coatings.

i.2 Research Objectives

The primary goal of this research is twofold. On one hand, it aims to study the deposition of different materials using the PVD technique, collecting experimental data on mono- and multi-component thin films, with particular attention to the morphology, homogeneity, and overall quality of the resulting coatings. On the other hand, the research seeks to analyze in detail the performance of the custom-designed PVD machine developed by Professor Murakami, assessing its advantages, limitations, and efficiency under various operational conditions.

The possibility of combining multiple materials in a single process and precisely controlling deposition parameters offers a significant opportunity for optimizing functional coatings, not only in the nuclear field but also in high-tech industries such as aerospace and microelectronics [4]. Furthermore, the study of this internally developed machine provides an original contribution to the understanding of non-conventional PVD systems, paving the way for future advancements in terms of customization, versatility, and process efficiency.

Thus, the work contributes to broader progress in materials science and process engineering, offering data and methodologies valuable to both the scientific community and advanced industrial applications.

i.3 Thesis Structure

This thesis is structured into two main chapters, each addressing a specific aspect of the research.

The first chapter is theoretical and provides an introduction to the issues related to the resistance of materials used in the nuclear industry. It examines the primary degradation phenomena due to neutron, ion, and electron irradiation, highlighting the effects on microstructure and mechanical properties. It also presents an overview of

protective film deposition methods. Finally, it introduces the tools used for material analysis and characterization, including Scanning Electron Microscopy (SEM), optical microscopy, the nanoindentation machine, and the film deposition equipment.

The second chapter describes the experimental work carried out in the laboratories of the University of Tokyo. This section details the sample preparation process, the deposition techniques employed, and the experimental parameters used. It then presents the results of the analyses conducted on the treated materials, with particular focus on the operational performance of the deposition machine. Finally, a critical discussion of the obtained results is provided, highlighting the implications for the applicability of protective films in the nuclear industry and outlining possible future developments of the research.

With this structure, the thesis aims to provide a comprehensive and detailed overview of the work carried out, combining rigorous theoretical analysis with an extensive experimental section based on concrete data. The goal is to contribute to the understanding of degradation mechanisms in nuclear environments and to propose innovative solutions to enhance material performance.

Chapter 1: Theoretical Foundations and Analytical Tools

1.1 Issues with Materials in Nuclear Environments

The nuclear environment, whether for power generation in reactors or for other nuclear-related technologies, poses a significant challenge to the materials used in structures, components, and control systems. Materials exposed to nuclear radiation must endure a range of phenomena that can compromise their performance, durability, and safety. Research aimed at addressing these issues is therefore essential to ensure the efficiency and safety of nuclear installations.

Materials in nuclear environments are exposed to various types of radiation, including thermal and fast neutrons, photons, and charged particles such as protons and ions. Their interaction with matter induces a series of effects that result in physical damage, chemical changes, and alterations in the mechanical and electrical properties of the materials [1] [2].

1.1.1 Effects of Irradiation on Materials

The impact of radiation on materials strongly depends on two main factors: the type of particle involved in the energy transfer and the total radiation dose absorbed by the material. Before analyzing the specific differences between various radiation sources, it is useful to outline the main effects that occur when materials are exposed to radiation.

One of the most relevant phenomena is swelling, which consists of volume expansion due to the accumulation of point defects, particularly vacancies, within the material. This effect can severely compromise the structural integrity of components, especially in applications where dimensional stability is critical, such as in nuclear reactors.

Another significant effect is radiation-induced creep, a plastic deformation that occurs under constant mechanical loads due to the progressive accumulation of irradiation damage. Unlike thermal creep, this process is accelerated by the interaction between mechanical stress and radiation-induced defects, leading to a reduction in mechanical strength over time.

Lastly, nuclear transmutation is a specific effect of neutron irradiation, whereby some of the constituent elements of a material are transformed into others due to nuclear reactions. This alters the original chemical composition, introducing new atomic

species that can significantly modify the material's physical and mechanical properties, affecting durability and overall performance.

If not properly controlled, these effects can severely limit the functionality of materials in irradiated environments, making the development of radiation-resistant alloys and composites crucial for advanced nuclear applications.

1.1.2 Degradation Induced by Ion Irradiation

Ions, being charged and relatively massive particles, interact strongly with the matter they traverse, triggering various transformations that may impair the structural and functional performance of materials. The main consequences of ion irradiation are listed in the following.

Displacement Damage

The interaction between energetic ions and target materials can transfer enough energy to overcome the atomic displacement threshold, causing atoms to be ejected from their lattice sites. This leads to the formation of structural defects at different scales. Microscopically, point defects such as vacancies and interstitials are created, disrupting the crystalline order. As the irradiation dose increases, these simple defects cluster into more complex configurations. These structural changes affect the macroscopic mechanical properties of the material, often resulting in increased brittleness and radiation hardening, which alter its behavior under mechanical stress. Understanding these mechanisms is crucial for predicting and mitigating radiation damage in materials for extreme environments.

Amorphization

At high doses, the accumulation of defects may result in the loss of crystalline order, transforming the material into an amorphous phase. This is especially problematic in ceramics and protective coatings used in nuclear components.

Chemical Alterations

The interaction between materials and ion beams can lead to significant modifications in surface and subsurface chemical composition. One of the most relevant phenomena is sputtering, a surface erosion process in which ion impacts eject atoms from the target material, particularly lighter elements [5]. Concurrently, ion implantation introduces foreign atomic species into the material's structure, altering its chemical composition and physical properties locally

These mechanisms are particularly relevant in fusion reactors, where internal walls are subject to intense bombardment by hydrogen and helium ions. The accumulation of these light particles can trigger severe structural degradation phenomena. Among

them, blistering is a critical issue: ions penetrating the material form gas bubbles beneath the surface, which expand and cause visible surface blistering and cracking.

Even more critical is delamination, the progressive separation of material layers. This occurs particularly in composites and multilayer systems and is caused by the buildup of internal stresses induced by irradiation. Delamination can irreversibly compromise structural integrity, drastically reducing the service life and safety of components. These effects represent one of the major engineering challenges in designing radiation-resistant materials for fusion reactors.

1.1.3 Effects of Electron Irradiation

Electrons, due to their much lower mass compared to ions, interact with matter mainly through ionization processes rather than atomic displacements. Nevertheless, under prolonged exposure, electrons can also cause significant structural damage.

Ionization and Electronic Modifications

The interaction between high-energy electrons and matter can trigger a range of complex physico-chemical processes. Energetic electrons may displace atomic electrons, initiating cascades of secondary effects: atoms become excited, electronic rearrangements occur, metastable states are formed, or surface chemical reactions are triggered.

These processes lead to notable changes in the material's fundamental properties. Specifically, alterations in electrical conductivity and charge carrier mobility are observed, along with variations in optical properties such as light absorption and emission. In semiconductors used in reactor monitoring and control systems, this can lead to progressive performance degradation, compromising the reliability of exposed electronic devices [6].

Radiation-Induced Damage

At high energies, electrons may cause damage similar to that caused by ions, particularly in organic materials and polymers used for electrical insulation. Electron irradiation is especially relevant in fission systems, where electronic components may experience a steady degradation of their functional properties, impacting system safety and reliability.

1.1.4 Degradation Induced by Neutron Irradiation

Neutrons, particularly fast neutrons, represent a major factor in the degradation of materials in nuclear environments. Neutron interactions with atomic nuclei trigger a variety of nuclear reactions, potentially resulting in the formation of radioactive

isotopes and the emission of secondary particles such as protons and electrons. These secondary emissions further contribute to material damage through additional radiation effects.

Both fast and thermal neutrons can alter the crystal structure, lattice integrity, and microstructure of materials, introducing defects that degrade their mechanical, thermal, and electronic properties. Such irradiation-induced damage can reduce mechanical strength, lower thermal conductivity, and impair electronic performance, thereby increasing the risk of failure or malfunction in components exposed to nuclear environments.

1.1.5 Degradation Induced by Ion and Neutron Irradiation

Simultaneous exposure to ions and neutrons is one of the primary degradation mechanisms in materials used in nuclear environments. These energetic particles interact with the structure of materials through different but equally harmful mechanisms. Neutrons, due to their high penetration ability, induce widespread atomic-scale damage throughout the material volume. Ions, on the other hand, deposit energy mostly in surface layers, creating highly localized but intense changes in properties.

The simultaneous exposure of materials to both neutrons and ions leads to compounded, multi-scale degradation phenomena. While the individual effects of each particle type have been discussed previously, their combined action can accelerate damage accumulation and exacerbate structural and chemical alterations. The presence of multiple irradiation sources can intensify swelling, radiation-induced creep, and nuclear transmutation, potentially reducing material lifetime and performance more rapidly than single-particle irradiation. This highlights the need to evaluate materials under combined irradiation conditions to accurately predict their behavior in realistic nuclear environments.

1.1.6 Combined Effects of Neutrons, Ions, and Electrons

In advanced nuclear reactors, particularly in fusion systems, structural materials are exposed to an extremely complex irradiation environment, characterized by the simultaneous presence of neutrons, ions, and electrons. This combination of energetic particles generates interconnected effects that often reinforce one another, resulting in more severe degradation phenomena compared to single-particle irradiation scenarios.

One of the most significant aspects is the synergistic effect of dual irradiation. Neutrons, with their high kinetic energy, are primarily responsible for the widespread creation of lattice defects, generating vacancies and interstitials on a microscopic scale. These displacement damages are further amplified by the action of ions, which

increase the dislocation density and promote the formation of defect clusters. At the same time, electrons interact with the material's electronic structure, altering its physico-chemical properties and making it more susceptible to additional damage mechanisms.

The temporal evolution of defects under these conditions is particularly critical. In fusion reactors, for instance, high-energy neutrons initiate the formation of primary defects, while hydrogen and helium ions, originating both from nuclear reactions and direct implantation, migrate toward these defects, accumulate, and form gas bubbles that lead to swelling and embrittlement. Simultaneously, electrons modify the interactions among defects, influencing their mobility and aggregation behavior, thereby altering the material's mechanical properties.

These combined phenomena present unprecedented engineering challenges for future fusion reactors, where both radiation flux and exposure time will be significantly higher than in current systems. Advanced studies that simulate multiparticle irradiation and investigate degradation mechanisms at the atomic scale are essential for progress toward more efficient and durable nuclear reactors.

1.1.7 Environmental Differences Between Nuclear Fission and Fusion

When analyzing material degradation phenomena in nuclear applications, it is essential to consider the substantial environmental differences between fission and fusion reactors. Although both systems share some characteristics, they present distinct challenges in terms of radiation–material interactions.

In fission reactors, neutron irradiation is predominant and constitutes the primary source of damage to core materials. However, the role of electrons should not be overlooked. While less energetic, electrons significantly contribute to the degradation of electronic components and insulating materials. These charged particles can alter the electrical properties of semiconductors and dielectrics, potentially compromising the operation of control and safety systems.

Fusion environments, on the other hand, are even more extreme, featuring not only intense neutron fluxes, but also significant bombardment by light ions, primarily hydrogen and helium. These particles, generated through fusion reactions, interact with the first wall, penetrate the crystalline structure of materials, and accumulate as gas bubbles. Combined with the high operational temperatures typical of fusion reactor, this accelerates the diffusion of lattice defects, leading to a more rapid evolution of radiation damage.

The increased complexity of the fusion environment demands materials with exceptional performance [7], able to withstand a combination of severe conditions.

These include displacement damage induced by neutron irradiation, the accumulation of gases such as hydrogen and helium within the material structure, cyclic thermal and thermomechanical stresses, and potential corrosion or interactions with the plasma.

This environmental differentiation explains why materials developed for fission are often not directly transferable to fusion systems, and why materials research for fusion represents one of the most demanding frontiers in nuclear materials science.

1.1.8 Need for Protection with Thin Films

Given the nature of irradiation-induced damage, the need to protect sensitive materials from such destructive effects becomes clear. One of the most promising solutions is the use of protective thin films, which act as barriers against ionizing radiation. Thin films made of radiation-resistant materials can reduce the impact of radiation damage on the underlying substrates, thereby extending the service life of both structural and electronic components and improving their reliability in nuclear environments.

Moreover, adopting protective thin films allows for the preservation of electronic device performance even under extreme radiation exposure, by preventing the formation of structural defects that would compromise material functionality. The choice of thin film materials depends on the specific application requirements, the type of radiation expected, and the damage tolerance of the candidate materials.

In this study, the protective films fabricated in the laboratory were composed of a range of elements, including aluminum (Al), hafnium (Hf), titanium (Ti), vanadium (V), zinc (Zn) and zirconium (Zr).

The selection of these materials is driven by the distinct and complementary properties that each element contributes to the overall coating system. These materials were chosen with the goal of enhancing the film's mechanical integrity, thermal stability, and resistance to radiation-induced damage, essential requirements for materials exposed to the extreme conditions of nuclear environments.

Aluminum contributes by significantly reducing the overall density of the alloy while improving oxidation resistance. Its native oxide, Al_2O_3, is a robust passivation layer that forms rapidly and protects underlying material from further oxidation. Although aluminum has a relatively low melting point compared to other transition metals, its inclusion in the alloy matrix can improve the corrosion resistance and thermal stability of the protective film without severely compromising mechanical strength

Hafnium plays a critical role due to its exceptionally high thermal neutron absorption cross-section (around 2000 barns), making it effective in neutron shielding and flux moderation. Furthermore, it forms stable and refractory oxides such as HfO_2, which provide excellent resistance to oxidation and thermal degradation. These

characteristics make hafnium highly suitable for use in components exposed to prolonged irradiation and elevated temperatures.

Titanium enhances the mechanical properties of the coating, offering high strength-to-weight ratio and good corrosion resistance. Titanium oxides contribute to the stability of the passive film, and its presence in the alloy improves resistance to hydrogen embrittlement, a major concern in nuclear systems, especially in light water reactors.

Vanadium is included for its ability to improve ductility and high-temperature performance. It also exhibits low neutron absorption, which is desirable in materials used near fuel cladding. Vanadium forms stable solid solutions and contributes to the toughness and strength of the protective layer while maintaining a relatively low activation under neutron irradiation.

Zinc, although not traditionally associated with nuclear materials, can play a role in modifying the surface properties of the coating and enhancing its adhesion to the substrate. Its oxides may contribute to corrosion resistance, and in multicomponent systems, zinc can act as a sacrificial element that preferentially oxidizes, thus protecting the more critical structural elements of the film.

Zirconium is perhaps the most established nuclear structural material among the selected elements. It is widely used in the nuclear industry, especially in cladding applications, due to its excellent corrosion resistance in high-temperature water and its extremely low thermal neutron absorption cross-section. Zirconium alloys such as Zircaloy have long been employed in pressurized water and boiling water reactors. In the context of a multicomponent film, zirconium helps reinforce corrosion resistance and thermal stability. It also contributes to the mechanical integrity of the film, forming strong solid solutions and protective oxides (ZrO_2) that resist radiation damage and thermal degradation.

The combination of these elements in a single film is expected to produce a material with superior performance compared to conventional coatings. The concept of high-entropy alloys or compositionally complex alloys (CCAs) underlies this approach: by mixing multiple principal elements, the resulting film may benefit from high configurational entropy, leading to the formation of simple solid solution phases with enhanced mechanical properties and radiation tolerance [8] . Such alloys are also known to exhibit sluggish diffusion kinetics, which can help reduce defect migration and radiation-induced swelling.

For example, Zirconium, provides exceptional corrosion resistance in high-temperature water and possesses a very low thermal neutron absorption cross-section, making it ideal for use in fuel cladding and structural components. When combined with

hafnium, an element renowned for its high neutron capture capabilities, zirconium establishes a balanced film that both shields against neutron flux and maintains structural integrity under irradiation [9].

The following chapters will explore the characteristics of HEAs, the deposition and characterization techniques used for these thin films, and their effectiveness in enhancing material resistance under nuclear conditions.

1.2 High Entropy Alloys (HEAs)

High Entropy Alloys (HEAs) represent one of the most significant innovations in materials science in the past two decades. Unlike conventional alloys, which are typically based on one or two principal elements with minor additions of others, HEAs are composed of five or more elements in nearly equiatomic proportions. This unique configuration exploits the high mixing entropy to stabilize simple crystal structures such as face-centered cubic (FCC), body-centered cubic (BCC), or hexagonal close-packed (HCP), while avoiding the formation of brittle intermetallic phases that often compromise the mechanical properties of traditional alloys [10].

There is growing interest in these materials, particularly in the nuclear industry [11], where extreme operating conditions, high temperatures, intense neutron radiation, corrosive environments, and prolonged mechanical stress, demand alloys with superior performance compared to those currently available. Austenitic steels, for example, though widely used in reactors, progressively degrade due to irradiation-induced swelling and embrittlement. Similarly, zirconium-based alloys, used as cladding for fuel rods, are susceptible to hydrating and failure under accident conditions, as demonstrated in the Fukushima disaster.

In this context, HEAs emerge as ideal candidates for advanced nuclear applications due to their exceptional radiation damage resistance, thermal stability, and corrosion resistance. This section explores the scientific foundations of these materials, the rationale behind their development, their potential advantages in nuclear applications, and the challenges that must still be overcome for their widespread adoption.

1.2.1 Definition and Basic Principles

The fundamental concept behind HEAs is high configurational entropy, which favors the formation of homogeneous solid solutions. From a thermodynamic perspective, the mixing entropy in a multi-element alloy reaches sufficiently high values to stabilize simple crystalline structures, even in the absence of a dominant element. This behavior contrasts with traditional alloys, where a primary element (such as iron in steels or

nickel in superalloys) dictates the crystalline structure, while the remaining components are added in small amounts to tailor specific properties.

One of the most studied examples is the CoCrFeMnNi alloy [12], also known as the Cantor Alloy, which exhibits a stable FCC structure despite consisting of five different elements. Its homogeneous microstructure contributes to a unique combination of mechanical strength and ductility, characteristics that are difficult to achieve with conventional alloys.

1.2.2 Strengthening Mechanisms and Thermal Stability

In addition to the entropic effect, HEAs benefit from other phenomena that enhance their performance. One such mechanism is lattice distortion, caused by atomic size differences among the constituent elements. This distortion introduces internal stresses that hinder dislocation motion, thereby increasing the material's mechanical strength.

Another key aspect is the slow diffusion effect, referring to the reduced atomic mobility resulting from the compositional complexity. In conventional materials, high diffusivity at elevated temperatures can lead to undesirable phenomena such as grain growth or the precipitation of brittle phases. In HEAs, however, diffusion is slower, ensuring greater microstructural stability even under prolonged thermal exposure.

1.2.3 Limitations of Current Materials

The nuclear industry has long relied on materials such as austenitic stainless steels and zirconium alloys, which nonetheless present several critical issues in high-irradiation environments. Steels, for example, are subject to swelling, leading to volumetric expansion and embrittlement. Zirconium alloys, despite their excellent neutron absorption cross-section, are prone to chemical degradation when exposed to high-temperature water. At elevated temperatures, zirconium reacts with water to form zirconium oxide (ZrO_2) and hydrogen gas according to the reaction:

$$Zr + 2H_2O \rightarrow ZrO_2 + 2H_2$$

This reaction is highly exothermic, releasing significant heat that can accelerate further oxidation and material degradation. The formation of zirconium hydrides within the alloy also embrittles the cladding, reducing its mechanical strength and structural integrity. Moreover, the hydrogen produced during oxidation can accumulate in confined spaces, creating a serious explosion hazard if its concentration exceeds flammable limits. This combined effect of thermal, chemical, and mechanical degradation makes zirconium alloys vulnerable under accident conditions.

1.2.4 Potential Advantages of HEAs

High Entropy Alloys offer several properties that make them particularly suitable for use in nuclear reactors. One of the most significant is their outstanding resistance to radiation damage. Due to the complexity of their crystal lattice, radiation-induced defects such as vacancies and interstitials exhibit reduced mobility, limiting the accumulation of damage. Some studies have shown that alloys such as CrMnFeCoNi experience significantly less irradiation-induced swelling compared to austenitic steels [12].

Another advantage is their corrosion resistance in oxidizing environments. In Pressurized Water Reactors (PWRs), for example, structural materials are constantly exposed to high-temperature and high-pressure water, conditions that promote oxide formation and surface degradation. Certain HEAs, such as AlCrFeCoNi, exhibit exceptional corrosion resistance, even outperforming the most advanced stainless steels [13].

1.2.5 Applications in the Nuclear Industry

High Entropy Alloys represent one of the most promising innovations for fission reactors, particularly in the area of fuel rod cladding. Currently, these rods are protected by zirconium alloys, but HEAs could offer significant advantages due to their superior resistance to hydrating and irradiation-induced damage. These properties would not only enhance material durability but also contribute to increased reactor safety by reducing the risk of failure during accident scenarios.

Beyond cladding, HEAs can also be used in core internal structures, such as support grids and components of the cooling system, where their combination of mechanical strength and thermal stability could extend plant lifetime, reduce the frequency of component replacement, and optimize maintenance costs.

In the fusion sector, where operating conditions are even more demanding, HEAs are considered ideal for critical components such as the first wall and divertor, which are exposed to intense neutron fluxes and high-energy plasma. The ability of these materials to withstand extreme temperatures and energetic particle bombardment makes them prime candidates for next-generation reactor technologies such as ITER and DEMO [14]. The implementation of HEAs in these contexts could represent a decisive step toward the realization of safer, longer lasting, and more efficient nuclear fusion facilities.

1.3 Technologies for the Deposition of Protective Films

The deposition of protective thin films is a key strategy to enhance the resistance of materials used in extreme environments, such as nuclear settings. Coatings can protect against corrosion, oxidation, wear, and radiation damage. Deposition techniques are generally categorized into physical, chemical, and hybrid methods, each with specific characteristics that influence the quality and properties of the resulting films [15].

1.3.1 Physical Vapor Deposition (PVD)

Physical Vapor Deposition (PVD) is a widely used technique for producing thin coatings on various substrates, with applications in advanced technological sectors such as nuclear, electronic, and optical industries. PVD takes place in a high-vacuum chamber, which minimizes contamination by ambient gases or particles and improves film quality in terms of purity and adhesion to the substrate.

During the process, the material to be deposited, known as the target, is transformed into vapor phase through purely physical methods, without chemical reactions. Common techniques for vaporizing the target include resistive or electron beam heating, ion bombardment (sputtering) (Fig.1), and laser ablation [16]. This initial stage, called vapor generation, is critical for controlling the flow and composition of the emitted atoms or molecules.

Once generated, the vapor travels through the chamber toward the substrate in the material transport phase. Due to the near absence of pressure, the vapor travels in a straight line and reaches the substrate surface, where the final stage, condensation and film growth, occurs. Atoms orderly deposit on the surface, forming a thin film. The structural, mechanical, and chemical properties of the film depend on process parameters such as substrate temperature, residual pressure, kinetic energy of incident atoms, and the system's geometry.

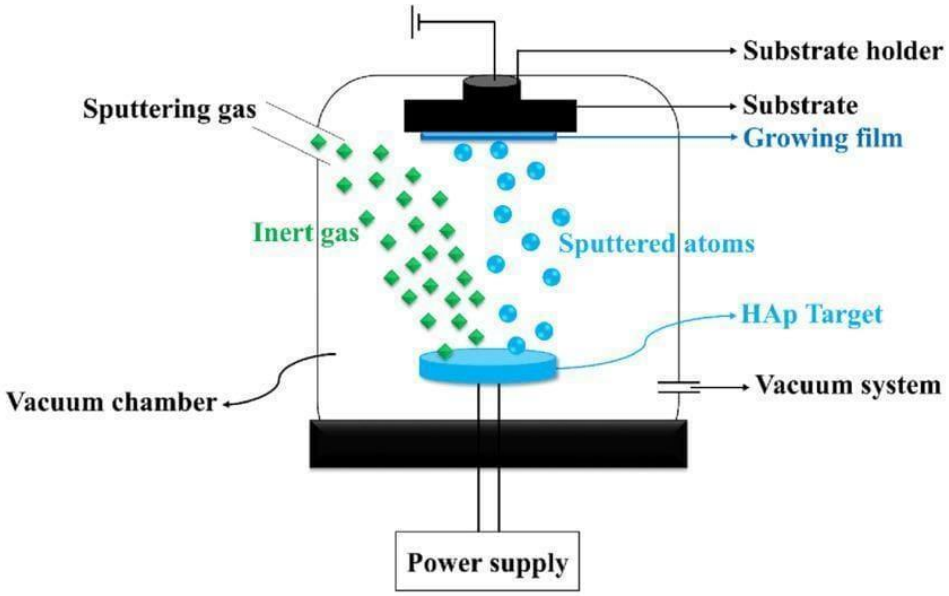

Figure 1: Schematic illustration of PVD deposition via sputtering (from [17]).

Thanks to its precision and versatility, PVD enables the fabrication of films with thicknesses ranging from nanometers to a few microns, with tailored properties ideal for protecting sensitive materials, improving wear resistance, or adding advanced functionalities to treated surfaces.

1.3.1.1 Applications of PVD

PVD technology is widely used across various industrial and scientific sectors due to its ability to produce advanced thin films with properties difficult to achieve through traditional methods. PVD films are characterized by strong adhesion, uniformity, high purity, and functional features such as resistance to wear, corrosion, oxidation, and high temperatures. These attributes make PVD highly versatile and strategic for applications demanding high performance and long-term reliability.

In the nuclear industry, PVD is employed to coat structural components exposed to extreme conditions such as intense radiation, chemically aggressive environments, and strong thermomechanical stresses. These coatings aim to extend material lifespan, reduce radioactive contamination, and improve corrosion resistance, ultimately contributing to plant safety and efficiency.

In the semiconductor industry, PVD is essential for manufacturing advanced electronic devices. It is used to deposit thin metallic conductive layers, such as aluminum, copper, or titanium, necessary for integrated circuits, transistors, and microelectronic components. In this context, nanometric precision and film purity are critical to ensuring reliable performance and device miniaturization.

The aerospace sector also benefits from PVD's capabilities, using it to enhance the mechanical and tribological properties of critical components such as turbine blades, bearings, and moving parts subject to high friction and wear. The coatings increase thermal fatigue resistance and extend material service life, reducing maintenance costs and improving flight safety.

In the medical field, PVD is used to produce biocompatible coatings for surgical instruments, implants, and prosthetics. These thin films not only improve corrosion resistance in biological environments but also reduce the risk of adverse reactions in patients, ensuring sterility, durability, and tissue integration. In some cases, coatings can be endowed with antibacterial properties or promote osseointegration, further expanding the technology's potential.

In summary, PVD is a key technology in fields where material reliability is crucial, enabling the development of advanced, customized solutions for the challenges of modern industry.

1.3.1.2 Advantages of PVD

PVD technology is widely adopted for producing high-purity thin films, thanks to its vacuum-based deposition process, which ensures superior quality and minimal contamination. One of its main advantages is the excellent adhesion of coatings to the substrate, enhancing durability and long-term resistance. Moreover, films produced via PVD, such as titanium nitride (TiN) or diamond-like carbon (DLC), exhibit exceptional hardness and wear resistance, making them ideal for applications requiring high mechanical performance.

Another strength is the ability to achieve uniform and precise coatings with nanometric thickness control, suitable even for high-tech applications. PVD's versatility allows for use with a wide range of materials, including metals, ceramics, polymers, and even glass, significantly broadening its application field.

However, this technology also presents notable disadvantages. One major limitation is the high initial and operational cost, stemming from the need for vacuum chambers and advanced plasma systems, which require complex maintenance. Furthermore, PVD may struggle to ensure uniform coverage on complex geometries, such as narrow angles or deep cavities, where coatings may be discontinuous.

Another limitation is the relatively slow deposition rate compared to other methods such as Chemical Vapor Deposition (CVD), which can be critical in industrial settings where productivity is key. Some PVD processes also operate at high temperatures, which may be unsuitable for heat-sensitive substrates. Lastly, if deposition parameters,

such as plasma or pressure control, are not optimized, microcracks or defects may form in the film, compromising its integrity and performance.

1.3.2 Chemical Vapor Deposition (CVD)

Chemical Vapor Deposition (CVD) is a widely used technique for producing high-performance thin films through controlled chemical reactions of gaseous precursors on a substrate surface [18]. The process occurs in a vacuum or controlled-pressure environment, with reaction energy supplied by heat, plasma, or laser depending on the variant. Precursors adsorb on the surface, react to form the solid film, and gaseous byproducts are evacuated.

Several CVD variants exist; each tailored to specific materials and applications. Thermal CVD (TCVD) relies solely on heat to drive chemical reactions, producing high-quality crystalline films; it is particularly suitable for substrates that can withstand temperatures of 600–1200 °C, ensuring dense, uniform coatings. Plasma-Enhanced CVD (PECVD) uses plasma to activate the reaction at much lower temperatures (200–600 °C), allowing deposition on thermally sensitive materials while improving film density and adhesion. Low-Pressure CVD (LPCVD) operates under reduced pressure (<150 Pa), promoting highly uniform films over large or complex surfaces and minimizing particle formation or defects, making it ideal for precise and large-scale coating applications.

Compared to PVD, CVD allows excellent conformality, chemical composition control, and high-purity films, especially on complex geometries. However, it generally requires higher temperatures, specialized precursors, and more complex equipment, increasing costs and safety concerns. PVD, by contrast, offers simpler deposition at lower temperatures and is highly versatile for metallic and alloy coatings, making it the preferred choice for the films studied in this work.

CVD is applied across multiple industries: in nuclear engineering, it deposits radiation-resistant coatings (e.g., SiC, B_4C); in microelectronics, it fabricates semiconductors; in aerospace, it produces wear- and heat-resistant surfaces; and in biomedical fields, it enhances implant biocompatibility. Its main advantages are high-quality, uniform, and adherent films, while limitations include temperature constraints, high cost, and precursor hazards.

1.3.3 Atomic Layer Deposition (ALD)

Atomic Layer Deposition (ALD) is a thin-film deposition technique that allows atomic-level control over thickness and composition [19] [20]. It relies on sequential, self-

limiting chemical reactions, depositing one atomic layer per cycle [20]. This ensures exceptional conformality and uniformity, even on complex or porous surfaces, making ALD ideal for microelectronics, nanodevices, and protective coatings in extreme environments. ALD films exhibit high density, low roughness, and excellent adhesion, which are particularly valuable when precise chemical or structural control is required.

However, ALD is relatively slow, as each cycle deposits only a single atomic layer, and it requires expensive equipment and highly pure precursors. These constraints make it less suitable for thicker coatings or larger substrates, common in nuclear materials research.

In comparison, PVD offers faster deposition rates and greater versatility for metallic and alloy coatings. While PVD may provide slightly less conformality than ALD, it produces dense, adherent films with tailored mechanical and radiation-resistant properties more efficiently. For these reasons, PVD was chosen for this work: it balances film quality, process speed, and adaptability, making it the preferred method for the production of protective coatings on nuclear materials.

1.4 Instrumentation Used for Analysis

The analysis of materials, especially those intended for nuclear applications, requires precise characterization of their morphological and structural properties. For this reason, advanced techniques such as Scanning Electron Microscopy (SEM), optical microscopy, and thin film deposition equipment are employed. Each instrument features specific characteristics that make it suitable for certain types of analyses, allowing for a comprehensive understanding of the materials being studied.

1.4.1 Scanning Electron Microscopy (SEM): Principles and Applications

Scanning Electron Microscopy (SEM) is one of the most powerful analytical tools for characterizing material surfaces at the microscopic scale. The SEM uses a high-energy electron beam to scan the surface of a sample, generating high-resolution images. The interaction between the electron beam and the sample produces various signals, such as secondary electrons, backscattered electrons, and X-rays, which are detected and used to construct a detailed image of the surface.

In the following section, all technical information regarding the scanning electron microscope is derived from the official JEOL documentation [21].

1.4.1.1 Operating Principles

The SEM consists of a vacuum column in which the electron beam is accelerated. This beam is focused into a fine spot and directed onto the sample surface. The interaction

between the electron beam and the sample generates several types of signals used to produce high-quality images.

Secondary Electrons:

Secondary electrons are low-energy particles emitted from the sample surface when struck by the primary electron beam. With kinetic energies generally below 50 eV, they are highly sensitive to surface topography. This makes them especially useful for producing detailed, high-resolution images of surface morphology. Images obtained from secondary electrons offer a three-dimensional view of the surface, clearly revealing features such as protrusions, cavities, porosity, and surface textures.

Backscattered Electrons (BSE):

Backscattered electrons are primary electrons that, after penetrating the sample, undergo elastic collisions with atoms in the material and are deflected backward. Unlike secondary electrons, they retain relatively high energy. Their intensity strongly depends on the chemical composition and atomic number of the sample, making them useful for compositional contrast imaging. For example, areas with higher atomic number elements appear brighter, allowing different materials within a sample to be distinguished.

Characteristic X-rays:

When an incident electron displaces an inner-shell electron from an atom, an electron from a higher energy level fills the vacancy, releasing energy in the form of an X-ray photon. This X-ray is characteristic of the emitting element, enabling chemical analysis. Techniques such as Energy Dispersive X-ray Spectroscopy (EDS or EDX) are used to identify and quantify elements in the analyzed area, providing accurate information on the elemental composition (Fig.2).

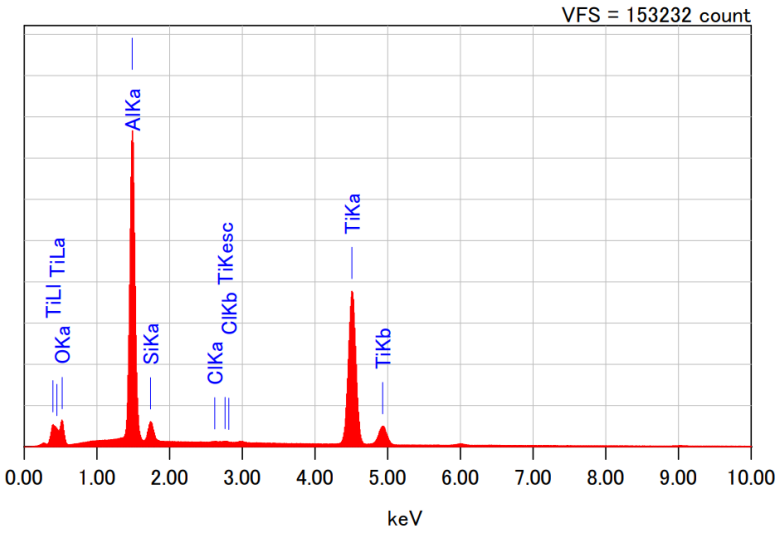

Figure 2: Example of an EDS spectrum, with X-ray energy on the x-axis and the corresponding counts on the y-axis.

As shown in the figure, it is easy to see that the main components of the surface are Al and Ti. Titanium peaks, for example, are labeled as Ti Kα and Ti Kβ, corresponding to X-rays emitted from electrons transitioning from the L and M shells to the K-shell, respectively. In this example, a certain amount of silicon from the substrate is also detected, indicating that the TiAl layer is not thick enough to fully shield the substrate. Additionally, traces of impurities such as oxygen and carbon are present, as commonly observed on samples. A small background error can also be noticed, visible as a general increase in counts at low energies, particularly between 1 and 2 keV.

1.4.1.2 SEM Structure and Main Components

Electron Beam Source

Generated by an electron gun and focused by electromagnetic lenses, the beam is directed onto the sample surface.

Scanning System

A magnetic coil moves the beam across the sample surface in a raster scan pattern, similar to how an image is read by a camera sensor.

Secondary Electron Detectors

These are the most commonly used detectors in SEM and are dedicated to collecting low-energy secondary electrons. Due to their sensitivity to surface morphology, they provide high-resolution images that reveal fine topographic features such as fractures, porosity, and texture (Fig.3).

Backscattered Electron Detectors

These detect high-energy primary electrons scattered backward after interaction with the sample. The number of detected BSEs depends on the sample's atomic number and density, making these detectors ideal for highlighting compositional differences within the sample.

X-ray Detectors

As the electron beam interacts with the sample, characteristic X-rays are emitted. Integrated EDS/EDX systems analyze these X-rays, enabling qualitative and quantitative

elemental analysis (Fig.2). This is essential for material identification and compositional studies.

Vacuum System

To prevent interference from air molecules, SEMs operate under vacuum, maintained by a vacuum pump system.

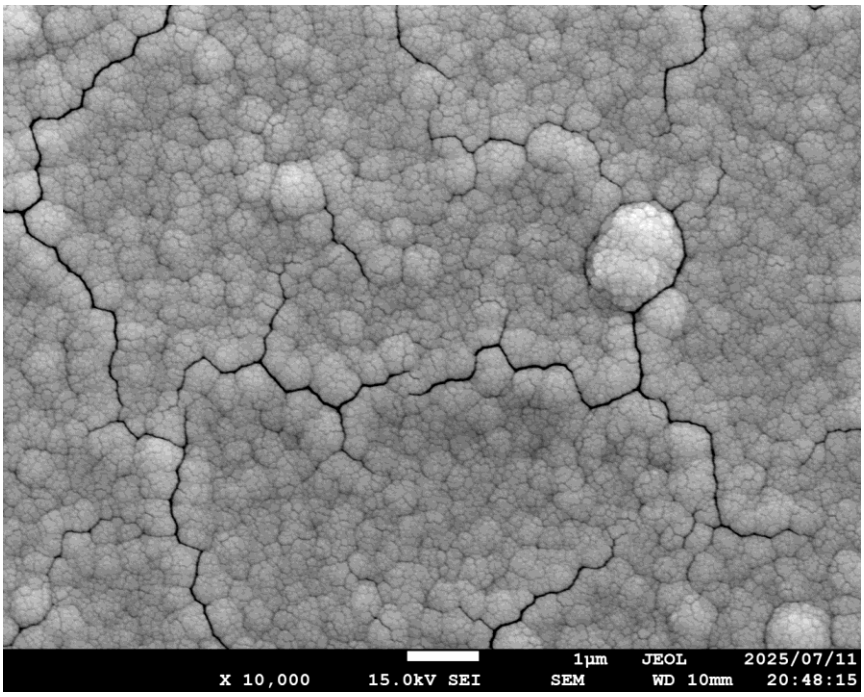

Figure 3: Example of an image acquired using the SEM (1 μm scale bar).

1.4.1.3 Advantages and Limitations of SEM

High Resolution:

A major advantage of SEM is its resolution, significantly superior to that of conventional optical microscopes. While optical resolution is limited by visible light wavelength, the electron beam allows resolutions down to the nanometer scale (Fig.3), enabling the observation of microstructures, defects, and fine surface features.

3D Surface Imaging:

SEM images exhibit strong three-dimensionality, due to the use of secondary electrons, providing clear insight into surface relief, depth, and inclination—making interpretation of complex surfaces intuitive.

Elemental Analysis:

Beyond morphological observation, SEMs equipped with EDS/EDX systems allow detailed chemical analysis of the sample area, making the instrument a complete tool for combined structural and compositional investigations.

Examination of Complex Surfaces:

SEM is ideal for irregular, porous, or geometrically complex surfaces, thanks to its high depth of field, which ensures clarity even on three-dimensional structures.

Limitations:

Sample Preparation

Non-conductive samples may accumulate charge under the beam, distorting images. These typically need to be coated with a conductive material (e.g., gold or carbon). Samples must also be dry and vacuum-stable, often requiring specific pre-treatment.

Lower Resolution than TEM

While SEM offers high resolution, it is still lower than that of Transmission Electron Microscopy (TEM), which can visualize atomic structures. This is because SEM is surface based, whereas TEM captures internal structural details.

Time and Cost

SEM imaging can be time-consuming, particularly at high resolutions or with compositional analysis. Equipment is costly, requiring complex maintenance and skilled operators. Sample preparation can also be demanding.

1.4.1.5 SEM SYSTEM USED

An example of a scanning electron microscope (SEM), used during this research, is the JSM-7001F manufactured by JEOL (Fig.4), one of the most advanced machines in the field of electron microscopy.

The JSM-7001F is a high-resolution SEM designed to provide detailed and accurate images, suitable for a wide range of scientific and industrial applications. Its main characteristics and technical specifications include:

The JSM-7001F scanning electron microscope stands out for its high performance, thanks to a series of advanced technical features that make it particularly suitable for morphological and compositional analysis of materials, including those used in the nuclear field.

Figure 4: SEM machine used

From a resolution standpoint, the machine is capable of providing extremely detailed images: in SE mode (secondary electrons), it can achieve a resolution of 1.0 nanometer at 15 kV, while in BSE mode (backscattered electrons) the resolution is 2.0 nanometers at the same voltage. These values allow for the analysis of surfaces at a nanometric level, revealing even the finest structures.

The system is equipped with an electron accelerator with a variable voltage ranging from 0.5 kV to 30 kV, which enables great flexibility in the analysis of various samples, both conductive and non-conductive. The highly focused electron beam ensures high precision in observing surface morphology.

A key element of this SEM is the field emission gun (FEG)-based lens system, which offers a more coherent and stable electron beam compared to traditional thermal guns. This results in sharper images with less noise, even at very high magnifications.

The JSM-7001F supports various imaging modes: SE mode, ideal for studying surface topography and morphology; BSE mode, which exploits differences in electron density to analyze the composition and internal structure of the sample; and EDS mode (Energy Dispersive Spectroscopy), which allows for compositional analysis by identifying chemical elements through X-ray emission.

Regarding compositional analysis, the SEM can be equipped with an integrated EDS system, which enables the collection of detailed chemical data on the sample. This functionality is particularly important in the study of nuclear materials, where precise knowledge of the composition is crucial.

The analysis area is large, with a maximum scan size of 30 mm × 30 mm, while maintaining high resolution. This is more than sufficient for our specimens, which measure 15 mm × 15 mm. Additionally, the sample can be positioned on a precisely adjustable stage, allowing the examination of different regions, including three-dimensional or irregularly shaped surfaces.

Finally, to ensure the accuracy of the analyses, the machine is equipped with a vacuum chamber that minimizes contamination from air and moisture, an essential aspect for sensitive samples. This is complemented by an advanced leak detection system, which ensures the constant maintenance of optimal vacuum conditions throughout the observation session.

Applications of the JSM-7001F

The JSM-7001F SEM is used in the laboratory to examine material morphology with high precision, making it particularly valuable for studying thin films employed as radiation-protective coatings. Its high-resolution SE imaging allows identification of surface defects, growth irregularities, and discontinuities that could affect the film's performance, providing critical information on deposition quality and material reliability.

The SEM's integration with energy-dispersive spectroscopy (EDS) enables precise elemental analysis. This is essential for nuclear materials research, allowing verification of coating homogeneity, detection of impurities, and assessment of the correct elemental distribution to ensure radiation resistance and chemical stability.

The instrument is also ideal for analyzing composite and multilayer materials. High-resolution imaging allows detailed study of interfaces, layer adhesion, and localized structural defects, which is crucial for developing coatings with tailored mechanical, thermal, or chemical properties for harsh environments.

Finally, the JSM-7001F is essential for monitoring material degradation under extreme conditions such as ionizing radiation or high temperatures. Surface observations reveal damage phenomena like cracks, porosity, or microfractures, providing insight into degradation mechanisms and guiding the development of more durable protective solutions.

Overall, the JSM-7001F is a versatile and powerful SEM, capable of detailed morphological and chemical analysis, making it an indispensable tool for laboratory research on nuclear material protection.

1.4.2 Optical Microscopy: Features and Usage

Optical microscopy is one of the most traditional and widely used techniques for observing samples at the microscopic level. It uses visible light to illuminate the sample and allows images of its morphological, structural, and, in some cases, functional characteristics to be obtained. Unlike electron microscopy, which uses an electron beam, optical microscopy is based on a beam of visible light or other electromagnetic radiation (such as infrared or ultraviolet light) that interacts with the sample.

In the following section, all technical information regarding the VK-X 3000 laser microscope is derived from the official Keyence manual [22].

1.4.2.1 Operating Principle

Optical microscopy is based on the law of light refraction. A sample is illuminated by a light source, and the light reflected or transmitted by the sample passes through a system of optical lenses that magnify it. This beam of light can be focused on the surface of the sample or pass through it, depending on the type of microscopy (e.g., bright-field, dark-field, or phase-contrast mode).

Main stages of the process:

The observation process through an optical microscope is structured in several fundamental stages that allow an enlarged and detailed image of the sample to be obtained. First is the illumination phase, in which a light source, usually a tungsten or mercury lamp, emits light that is directed through a condenser lens system. This system's role is to focus and evenly direct the light beam onto the sample, ensuring proper illumination for observation.

Next, the light interacts with the sample, and this interaction varies depending on the nature and structure of the material. Some wavelengths may be absorbed, while others may be refracted, diffracted, or transmitted. These physical phenomena generate optical contrasts that make it possible to distinguish different structures in the sample, revealing details not visible to the naked eye.

The light transmitted or reflected by the sample is then collected by a second lens system, which focuses it onto an observation plane. At this stage, the image is progressively magnified through the objective and the eyepiece or, in modern systems, projected onto a digital sensor for display on a monitor.

Finally, the actual observation phase takes place, where the final image is visible to the operator. Depending on the instrument's configuration, this can be viewed directly through the eyepieces or displayed and analyzed on a screen, enabling recording and digital processing of the data obtained.

1.4.2.2 Main Components of the Optical Microscope

The optical microscope is composed of several key elements, each of which plays an essential role in ensuring accurate and detailed observation of the sample. The process begins with the light source, which may consist of an incandescent lamp, a mercury lamp, or a xenon lamp, depending on experimental needs. The emitted light may belong to the visible spectrum, but also to ultraviolet (UV) or infrared, depending on the nature of the analysis and the type of contrast desired.

The light produced by the source is then directed toward the condenser, a lens system that focuses the light beam on the specific area of the sample to be observed. The condenser is crucial for optimizing illumination and directly influences the contrast and quality of the observed image. Proper positioning and adjustment of the condenser result in sharper and more detailed images.

After interacting with the sample, the light passes through the objectives, which are interchangeable lenses with various magnification factors, typically ranging from 4x to 100x. Objectives allow observation of structures with varying levels of detail based on the selected magnification. Each objective is designed to balance resolution and field of view, enabling gradual and thorough exploration of the sample.

The magnified image is then observed through the eyepiece, a lens located at the top of the microscope. The eyepiece provides additional magnification (typically 10x) and represents the direct observation point for the operator. In some modern configurations, the eyepiece may be replaced or complemented by a digital system, such as a camera or monitor, useful for shared observation or for recording and analyzing images.

The sample is placed on the stage, an adjustable platform that allows horizontal and vertical movement of the sample. This enables the exploration of different areas of the slide without removing it, facilitating the investigation of large sections or returning to specific points.

Finally, to obtain a clear and defined image, a focusing system is used, composed of two knobs: one for coarse adjustment and the other for fine adjustment. This mechanism allows precise regulation of the distance between the lenses and the sample, ensuring a sharp image at any magnification and compensating for variations in specimen thickness or height.

1.4.2.3 Types of Optical Microscopy

Bright-Field Microscopy:

This is the most common type of optical microscopy. Light passes through the sample, and the image appears as a dark projection on a bright background. This type is useful for observing transparent or stained samples, such as cells or biological tissues.

Dark-Field Microscopy:

In this mode, light does not pass directly through the sample but is directed so that only light scattered by the sample reaches the objective. The sample appears as a bright figure on a dark background. This technique is useful for highlighting small details or very thin structures, such as cell edges.

Phase-Contrast Microscopy:

Phase-contrast microscopy exploits the phase differences of light passing through the sample to create contrast without staining. It is useful for observing transparent biological samples, such as living cells, without damaging them.

Fluorescence Microscopy:

In this mode, the sample is labeled with fluorochromes (fluorescent dyes) that emit light when excited by a high-intensity light source. This type is particularly useful for studying the localization of specific components within cells or tissues, such as proteins, nucleic acids, etc.

Interference Contrast Microscopy:

This type is used to observe unstained samples and offers high contrast due to differences in the optical properties of the sample. It is especially useful for studying the fine structure of biological samples

1.4.2.4 Advantages and Limitations of Optical Microscopy

One of the main advantages of optical microscopy lies in its accessibility and ease of use. Compared to more complex techniques such as electron microscopy, optical microscopes are relatively simple to operate, making them suitable for a wide range of applications and users, including non-specialists.

Another significant advantage is its non-invasive nature. Optical microscopy allows for non-destructive observation of samples, even in real-time. This feature is particularly useful for studying dynamic biological processes or cellular behavior under natural conditions, without altering or damaging the specimens.

Additionally, with the appropriate configuration, optical microscopy is well-suited for observing living samples. Cells and microorganisms can be examined while remaining viable, which is essential for investigations that require monitoring physiological or metabolic activity.

Despite these benefits, optical microscopy also has some limitations. The most significant is its limited resolution. Compared to electron microscopy, optical systems are less capable of resolving fine structural details. The typical resolution limit is around 200 nanometers, which is well above the atomic scale and insufficient for visualizing ultrastructural or molecular-level features.

Furthermore, optical microscopy generally provides high-quality images of sample surfaces, but it is not able to produce high-resolution images of internal structures at the submicroscopic level. To overcome this limitation, advanced techniques such as fluorescence or confocal microscopy are required, which add complexity and require specialized preparation or equipment.

1.4.2.5 Optical Microscopy Applications

Optical microscopy is widely used in numerous fields of research and application due to its versatility and ease of use. In biology and medicine, it plays a fundamental role in the observation of cells, tissues, and microorganisms. It is employed in various biological studies, such as monitoring cellular processes, analyzing cell cultures, and diagnosing diseases—for example, through the examination of biopsies.

In the field of materials science and nanotechnology, although limited in resolution, optical microscopy remains a valuable tool for observing the surface structure of materials and devices at the microscopic scale. It allows researchers to examine surface morphology, detect defects, and monitor the effects of processing or treatment, all without the need for destructive testing.

Additionally, in pharmacy and chemistry, optical microscopy is used to study the morphology of powders, crystals, and various materials at a fine scale. These observations are essential for characterizing substances, understanding material properties, and optimizing formulations in pharmaceutical and chemical research.

1.4.2.6 Machine used

The advanced optical microscopy system used during this research is the VK-X 3000, a device produced by Keyence. This is a 3D scanning interference microscope that combines the capabilities of traditional optical microscopy with interferometric technology to obtain high-precision 3D images. The VK-X 3000 is particularly useful for analyzing the surface morphology of samples at the microscopic level, offering excellent resolution and the ability to visualize topography in great detail. The use of this machine can be especially relevant in the context of your research on silicon-based materials and other surfaces to be protected from radiation.

Figure 5: VK-X 3000 microscope used

Specifications of the VK-X 3000

The VK-X 3000 is a 3D optical interference microscope capable of acquiring high-resolution surface images without complex sample preparation, ideal for fragile or intricate specimens. It offers a vertical resolution of up to 1 nm and a magnification range from 5× to 500×, allowing detailed topography measurements across a wide variety of surfaces.

One of the most distinctive features of this machine is its capability to measure surface roughness with exceptional precision. This function is essential in applications such as the analysis of protective coatings. The integrated software allows for the calculation of roughness parameters such as Ra (arithmetical mean roughness), Rz (average peak-to-valley height), and other relevant indices, which can be used to evaluate the effectiveness of surface treatments.

The system is also capable of acquiring 3D surface images by collecting topographic data across multiple planes. This technology enables in-depth visualization and provides an accurate representation of the shape and characteristics of complex sample surfaces.

High-speed scanning enables rapid imaging and measurement, useful for analyzing multiple samples efficiently. Illumination is provided by a high-intensity LED, ensuring clear visibility without damaging the surface. Advanced analysis software processes

the acquired data, producing detailed measurements, roughness analyses, and graphical outputs.

Applications of the VK-X 3000

In our laboratory, the VK-X 3000 microscope is primarily used to analyze the surface topography and roughness of materials, with a focus on thin films and radiation-resistant coatings. Its high-resolution 3D imaging allows precise examination of silicon-based protective films, enabling the identification of surface defects, irregularities, and variations in thickness that could affect performance under irradiation or mechanical stress.

The system is particularly useful for studying samples with complex or irregular shapes, providing accurate representations of coated surfaces and interfaces. Roughness measurements are performed to assess the quality of deposited films and their ability to withstand experimental treatments such as ionizing radiation or thermal cycling.

Additionally, the VK-X 3000 supports monitoring the evolution of material surfaces during research experiments, allowing us to track degradation, defect formation, or changes induced by exposure to radiation or stress. This capability is essential for optimizing protective coatings and understanding the mechanisms that influence their durability.

Overall, the VK-X 3000 is a versatile and powerful tool in our laboratory, enabling detailed 3D analysis of surface morphology, roughness, and microstructure, which is critical for both quality control and advanced research on radiation-resistant materials.

1.4.3 Nanoindentation: Principles and Applications to Thin Films

Nanoindentation is an advanced technique used to characterize the mechanical properties of materials at the nanometric scale, including Young's modulus, hardness, and, in some cases, the Poisson's ratio. Unlike conventional mechanical testing methods, which require large samples, nanoindentation is particularly suitable for analyzing materials in the form of thin films, coatings, or microstructures.

The operating principle is based on the controlled application of a force via a penetrator (typically diamond) onto the sample surface, simultaneously measuring the penetrator displacement as a function of the applied load. Analysis of the loading-unloading cycle allows the extraction of the elastic and plastic properties of the tested material, according to the Oliver and Pharr method, which is currently the most widely used for interpreting nanoindentation data.

Figure 6: Nanoindentation machine used

All technical details regarding the operation and capabilities of the DUH-211 referenced in this work are based on the official Shimadzu manual [23].

1.4.3.1 Instrumentation and Experimental Setup

In this work, an instrumented nanoindentation machine was employed, equipped with a diamond Berkovich indenter featuring a triangular geometry with a tip angle of 65.3°. The resolution of the instrument enables measurement of vertical displacements on the order of nanometers and forces below the micronewton scale, making it suitable for characterizing thin films with micrometric thickness.

The sample under examination consists of a film deposited on a crystalline silicon substrate. To ensure the measurement reflects only the properties of the film without substrate influence, the commonly accepted criterion was followed, according to which the maximum penetration depth must be less than one-tenth of the film thickness. In our case, considering a film thickness of approximately 2 μm, the indentation depth was kept below 200 nm.

1.4.3.2 Considerations on Indentation Depth

Substrate influence is one of the main challenges when measuring the mechanical properties of thin films via nanoindentation. If the penetration depth is too large relative to the film thickness, the stress propagates into the substrate, altering the obtained results. In particular, the resulting elastic modulus would tend to represent a weighted average between the film material and the underlying substrate.

To avoid this effect, besides respecting the depth criterion (<10% of the film thickness), a preliminary analysis with tests at different depths was conducted to check for substrate effects. The obtained load-displacement curves were compared, and data

showing evident silicon influence were excluded (for example, in cases of anomalous stiffness increase during the elastic unloading portion of the curve)

1.4.3.3 Machine used

In this work, the mechanical properties of the thin films were evaluated using the Shimadzu DUH-211 machine (Fig.6). This instrument was selected for its ability to accurately measure the hardness of very thin films without damaging the surface, a capability that conventional macro- or micro-hardness testers cannot provide. Its high sensitivity and low-force resolution allowed precise assessment of the mechanical response of our 15 mm × 15 mm specimens, providing essential data on film integrity, adhesion, and uniformity.

The DUH-211 enabled the identification of variations in hardness across the film surface, highlighting potential deposition defects or inhomogeneities, which are critical for understanding the protective performance of the coatings under radiation or mechanical stress. By using this instrument, we obtained quantitative mechanical data that directly supported the evaluation of the films' suitability as protective layers in nuclear applications.

Figure 7: example of indentation with different force applied (1 µm scale bar).

Figure 7 shows the surface of a specimen after nanoindentation. In both cases, the critical role of the applied load is evident: deeper penetrations require higher forces, which may lead to material yielding and result in inaccurate measurements of the

mechanical properties. This effect is clearly visible in Figure 8, where excessive force causes noticeable surface deformation around the indentation.

1.4.4 Physical Vapor Deposition (PVD): Design and Operation of the Machine Developed in the Murakami Laboratory

Physical Vapor Deposition (PVD) is a widely used technique for producing thin films and coatings with controlled properties. It is based on the physical vaporization of the material to be deposited (the target), followed by its condensation on the substrate surface. The process typically occurs in a high-vacuum environment and uses an inert gas, generally argon, which facilitates the formation of the plasma required for the sputtering mechanism.

This technique is particularly effective for depositing metals, alloys, and ceramic materials on various types of substrates. In the context of this work, PVD was employed to create multicomponent films with advanced mechanical properties, which were subsequently characterized by nanoindentation.

1.4.4.1 Design and Features of the Murakami Laboratory PVD Machine

The machine used in this study is a PVD system custom-designed and built under the direction of Prof. Murakami, the laboratory leader. This machine is a unique prototype, not commercially available, designed to meet research needs for advanced materials intended for extreme applications, such as nuclear or aerospace fields.

A distinctive feature is the presence of three separate holders for the targets, each equipped with its own 200 W power generator. This configuration allows simultaneous deposition of three different materials, with independent control over each plasma parameters. Such a setup enables the synthesis of multilayer or compositionally graded films, essential for producing heterogeneous high-performance materials (for example, multielement alloys or High Entropy Alloys – HEAs)

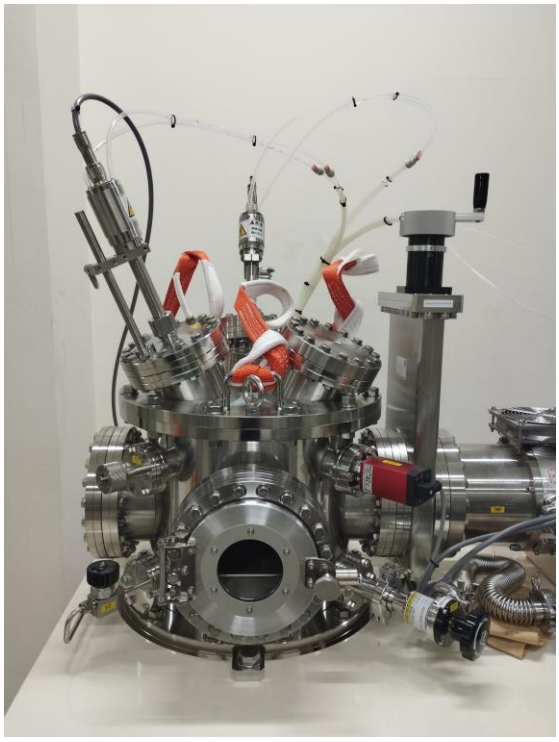

Figure 8: Front view of the PVD deposition system

1.4.4.2 Main Components of the Apparatus

Vacuum Chamber

The deposition chamber is made of stainless steel and is designed to operate under vacuum conditions that can exceed $10^{-6}\ Pa$. Its generous dimensions allow simultaneous accommodation of three targets.

Pumping System

The vacuum system consists of two pumps installed in series: a mechanical rotary pump used for rough vacuum, and a molecular pump capable of reaching pressures below $10^{-4}\ Pa$. This configuration ensures precise control of internal pressure, which is crucial for plasma stability and film quality. The pressure is continuously monitored by a high-sensitivity ion sensor, while the control system allows automatic adjustment of the inert gas flow rate.

Gas Injection (Argon)

The process gas injection system (argon) includes a mass flow controller (MFC) valve, ensuring reliable and precise flow regulation. Argon, being an inert gas, does not react with the targets and enables plasma generation necessary for sputtering by ion bombardment of the targets.

Cooling and Thermal Control System

During sputtering, targets can reach high temperatures due to continuous ion bombardment. To prevent material degradation and ensure stable deposition, each target is connected to a water-cooling circuit. This system includes a heat exchanger and a thermally controlled recirculation unit that maintains the operating temperature within a safe and constant range.

1.4.4.3 Plasma Generation and Process Parameters

Plasma generation is enabled by three 200 W DC generators, one for each target. This modular approach provides considerable flexibility in controlling plasma conditions for each material, which is crucial to optimizing deposition parameters for every individual element or alloy.

Argon introduced into the chamber is ionized by electrical power applications. The ions accelerated toward the targets cause sputtering, i.e., the ejection of atoms or atomic groups that then deposit onto the substrate. The chamber geometry and control of the target-substrate distance allow for homogeneous and well-adhered deposition.

Figure 9: Front view of the main control panel and operating settings

1.4.4.4 Advantages of the System and Applications

The unique design of the PVD machine developed in the Murakami laboratory enables controlled deposition of multicomponent materials and the synthesis of films with variable composition, such as compositional gradients or nanostructured layers. This

system also reduces processing times by allowing simultaneous depositions and ensures high reproducibility of the deposition parameters. These features make the system particularly well-suited for applications that require extreme customization of the deposited material, including coatings for nuclear components, materials for microelectronics, and films resistant to wear and corrosion.

Chapter 2: Experimental Results

2.1 Introduction

2.1.1 Chapter objective

The production of thin films on silicon substrates represents a crucial phase in the study of advanced materials for nuclear applications. In particular, within the framework of the present thesis, the films constitute the first experimental step in the exploration of lightweight High Entropy Alloys (HEAs), intended for subsequent evaluations of mechanical stability and resistance to irradiation-induced degradation. The ability to fabricate films with controlled composition, uniform thickness, and consistent microstructure is fundamental to ensuring the validity of the experimental data and their reproducibility.

This chapter aims to describe in detail the entire experimental process followed for the deposition of films on silicon substrates, highlighting the preparation steps, deposition configurations, design choices, operating parameters, and optimization strategies. The ultimate goal is to provide a robust and reproducible methodology suitable for the production of samples intended for the screening of multicomponent materials.

2.1.2 Overview of the Experimental Workflow

The experimental methodology adopted is based on the use of Physical Vapor Deposition (PVD), specifically through multi-target magnetron sputtering. This technique enables the production of films with controlled compositional gradients and high surface uniformity, making it particularly suitable for the fabrication of samples intended for screening studies of high-entropy materials.

A preliminary phase involved the use of substrate covering grids, aimed at modulating the deposition of materials from multiple targets and improving film uniformity. However, experimental tests revealed that the grids limited the freedom to generate compositional gradients along the substrate and complicated the management of multiple targets. Consequently, in the subsequent phases of the experiments, the grids were removed, while maintaining accurate control of the key deposition parameters. This choice allowed the production of samples with controlled compositional variations

across the surface, optimizing time and resources while providing an essential degree of freedom for the study of different elemental combinations within a single film.

2.1.3 Motivations and Experimental Relevance

The selection of silicon substrates, their preparation, and the deposition configuration represent fundamental steps for obtaining high-quality films. Chemical cleaning and surface treatment of the substrates were carried out following established protocols, with the aim of removing contaminants and surface oxides, and reducing roughness to values compatible with the requirements of uniform deposition.

Finally, the preliminary characterization of the films (thickness, chemical composition, and microstructure) constitutes an essential step for selecting the most promising samples for subsequent studies of mechanical behavior and irradiation resistance. The methodology developed therefore provides a solid and reproducible experimental foundation, essential for systematically addressing the advanced experimental phase on high-entropy materials.

2.2 Substrate Preparation

The preparation of substrates represents a preliminary yet essential phase in the deposition of thin films. The quality and properties of the substrate significantly influence the adhesion, morphology, and mechanical characteristics of the deposited coating. For this reason, it is fundamental to ensure that the samples are appropriately selected, thoroughly cleaned, and preliminarily characterized prior to deposition. The procedures adopted are aimed at minimizing the presence of organic contamination, unwanted oxides, and surface defects, in order to obtain a uniform and reproducible basis for the subsequent experiments.

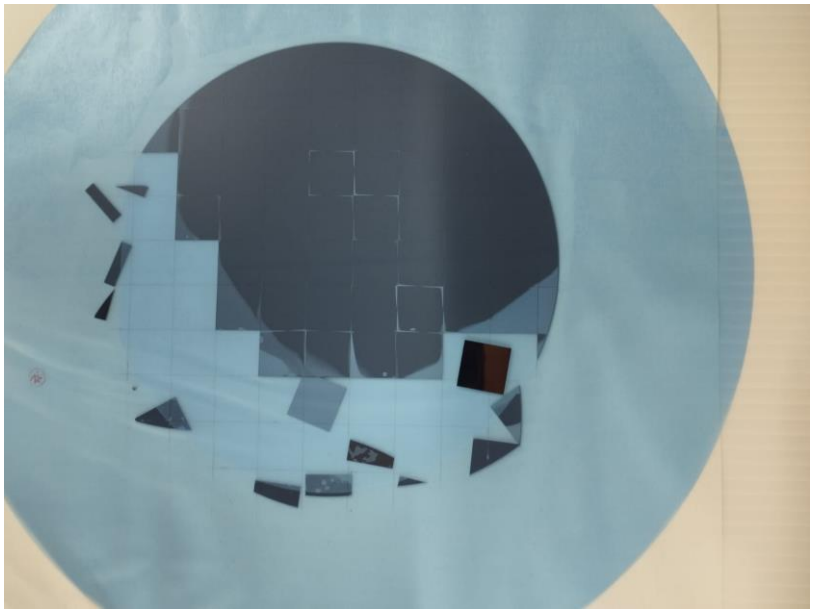

Figure 10: Silicon wafer cut and prepared for use (15 × 15 mm squares)

2.2.1 Type of Silicon Substrates

The substrates used in the experiments consist of monocrystalline silicon wafers, a material widely employed in both scientific and industrial contexts due to its availability, purity, and structural stability. Specifically, wafers with a crystallographic orientation of (100) were employed, selected for the different properties they provide in terms of response to deposition processes.

The thickness of the substrates is approximately 500 µm, a compromise that ensures mechanical stability during handling while remaining compatible with characterization techniques.

The choice of a specific crystal orientation is not purely technical, but responds to experimental needs related to film formation. For instance, silicon (100) tends to promote the growth of layers with a more regular morphology [24].

2.2.2 Chemical Cleaning and Surface Treatment

Once the substrates have been selected, it is necessary to remove all forms of surface contamination to ensure that deposition occurs on a clean and controlled surface. The most common impurities include organic residues from handling, native silicon oxides, and microscopic solid particles. The presence of such contaminants would compromise film adhesion and lead to a non-uniform distribution of the coating.

The substrates are subjected to washing with organic solvents, typically acetone and isopropanol, capable of removing oils and organic residues. In some cases, a thermal treatment (annealing) may also be applied to further stabilize the surface.

All these operations are conducted in a controlled environment, using dedicated gloves and tweezers to avoid recontamination.

2.3 Deposition Setup Selection and Optimization

The deposition of thin films requires careful selection of the experimental configuration, as the adopted parameters directly influence the coating quality and the reproducibility of the results. In the initial phase of this work, it was therefore necessary to analyze the main PVD techniques available, identify the most suitable configuration, and evaluate possible auxiliary tools to ensure uniformity and compositional control of the deposited film. The choices made in this preliminary stage significantly affected the subsequent phases, both from an operational and scientific point of view.

2.3.1 Overview of the PVD technique used

Physical Vapor Deposition (PVD) techniques represent a set of widely employed methodologies for the production of thin films on solid substrates. In this work, two main configurations were considered: magnetron sputtering and thermal evaporation.

Magnetron sputtering is based on the ejection of atoms from a target through ion bombardment in a plasma environment. This technique provides a high degree of control over the chemical composition of the film, enables the deposition of uniform coatings even on extended surfaces, and allows the fabrication of multicomponent alloys. In the context of high-entropy alloys, sputtering is particularly advantageous due to the possibility of simultaneously combining multiple metallic targets.

2.3.2 Need for coverage and types used

Another fundamental motivation for the use of coverage above the specimen concerns the measurement of the film thickness. The optical characterization techniques employed require the presence of a non-coated reference region in order to compare the optical properties of the bare substrate with those of the area covered by the film. Without a portion of exposed silicon, free from deposition, it would be impossible to accurately determine the coating thickness. For this reason, the use of partial masks or cover grids proved to be not only functional to deposition modulation but also strictly necessary to ensure correct measurement of the film’s fundamental parameters.

During the experimental phase, three different types of coverage were employed (Fig.11), each with specific characteristics:

1. Handmade aluminum foil: manually crafted from a thin aluminum sheet, cut, bent, and rolled to obtain the design shown in the figure.
2. Punctuated sheet grid: a thin plate with regularly spaced holes across the surface.
3. Mesh grid: composed of an interwoven metallic wire structure, providing an even denser control of the deposition, generating a high density of distinct regions on the substrate surface.

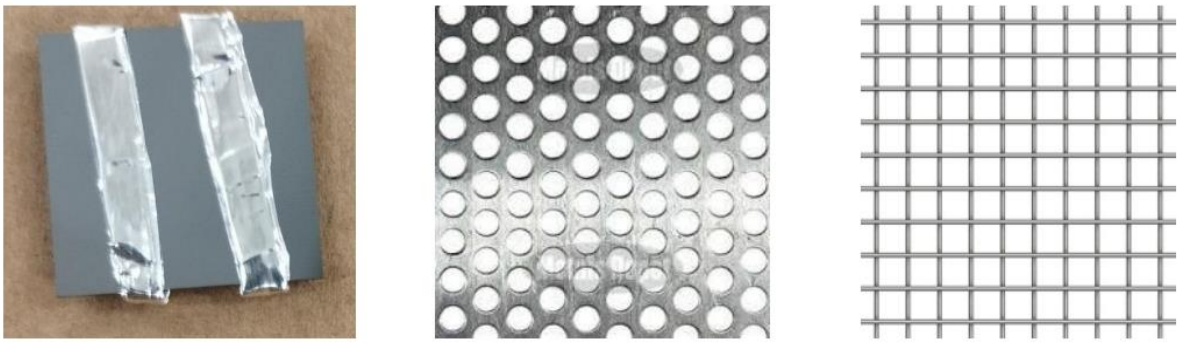

Figure 11: Types of coverage employed

2.3.3 Preliminary phase with coverage grids

A crucial aspect of this study was the use of coverage grids, introduced with the aim of modulating the deposition process and investigating in more detail the distribution of materials on the substrate. The grids, placed on the specimen surface, played a dual role, becoming a central element in the analysis and understanding of the properties of the obtained films.

The first motivation behind their use lies in the possibility of subdividing the specimen into a large number of discrete zones. By considering each of these areas sufficiently small, the film's composition and thickness can be approximated as constant within the same region. In this way, every portion of the surface is treated and analyzed as if it were an independent sample, enabling the creation of a detailed map of the coating's properties under nominally identical deposition conditions. This approach allows the investigation of a wide range of compositional configurations within a single deposition, thus maximizing experimental efficiency.

The second motivation relates to the management of surface diffusion phenomena. The introduction of a grid above the specimen aims at reducing or even preventing diffusion

along the surface plane, a phenomenon that, under standard conditions, tends to homogenize composition and microstructure. In this study, such homogenization was undesirable: the main goal was in fact to obtain slight inhomogeneity across the surface, so as to reproduce in a single sample different compositional and microstructural conditions. The grid, by limiting the lateral mobility of deposited atoms, preserves the local differences originating from the fluxes of the various targets, giving rise to controlled and reproducible compositional gradients.

The use of grids thus enabled the achievement of a dual result: on the one hand, creating a sample surface that could be subdivided into multiple areas equivalent to independent specimens; on the other, preserving compositional variations across the plane, avoiding excessive homogenization caused by atomic diffusion. This configuration enabled the development of an innovative experimental approach, in which coating diversity was not a limitation but rather an integral part of the investigation strategy.

2.3.4 Observed criticalities and decision to eliminate grids

Despite the initial advantages, the use of grids revealed two fundamental issues already in the early deposition stages.

The first problem concerned the non-uniformity of deposition within the uncovered areas. During the process, the film remains in a liquid state before cooling and solidifying. In this transitional phase, adhesion forces between the film and the metallic grid led to the formation of a meniscus (Fig. 12), altering the material distribution. The consequence is an irregular build-up at the edges of the uncovered region and significant internal non-uniformity. Moreover, the subsequent removal of the grid breaks the deposition edges, causing a loss of deposited material. This phenomenon not only damages coating continuity but also slows down the deposition rate, thus reducing the overall process efficiency.

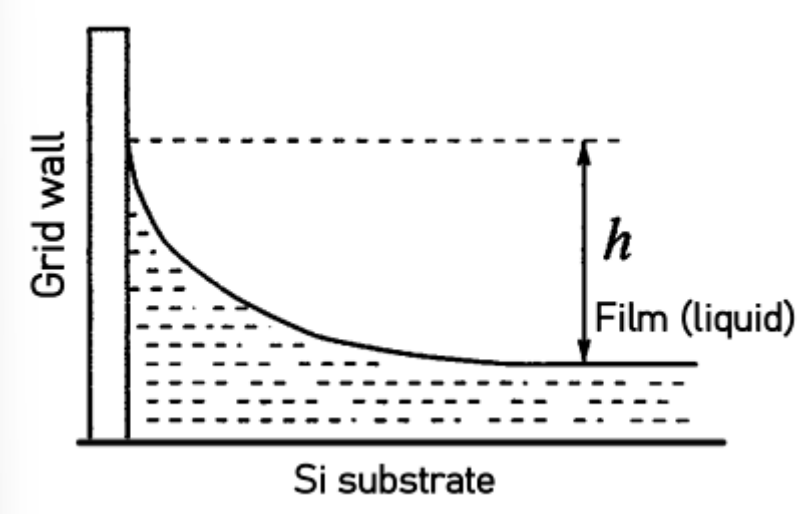

Figure 12: Non-uniform deposition

The second issue, which proved particularly critical and ultimately led to the grid's unsuitability, was the widening of the deposition area. As illustrated in Figure 13, the coating gradually extended beyond the grid's openings, spreading beneath their edges. This effect resulted in a further decrease in the average thickness, since the deposited material was redistributed over a larger surface than anticipated. During longer deposition times, the problem became even more severe: regions that were initially separated by the grid meshes expanded until they overlapped, generating an undesired continuity between areas that were expected to remain distinct.

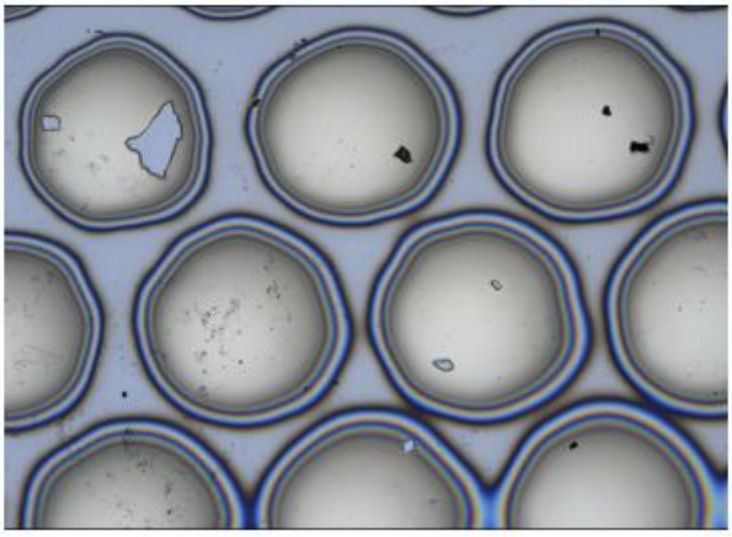

Figure 13: Deposition permeation under the grid wall (100 µm scale bar)

This issue proved particularly severe, as it prevented the formation of a bare silicon region required for optical thickness measurement. The lack of such a reference made

specimen characterization impracticable, compromising the entire deposition objective.

2.3.5 Results on grid performance

The next step was to quantify the material loss caused by grid use in order to assess whether they could be employed under the operational conditions of the selected deposition system. Comparisons were made using as a reference a specimen covered only by an aluminum foil and deposited with an Al 70% Ti 30% alloy, since this configuration was not expected to be affected by the undesirable phenomena described above. To this end, one sample was prepared with this coverage, three specimens with punctuated sheets, and one with the mesh grid. The latter, however, was immediately discarded, as the quadrants that should have remained separated eventually overlapped, generating a surface unsuitable for quantitative analysis (Fig. 14).

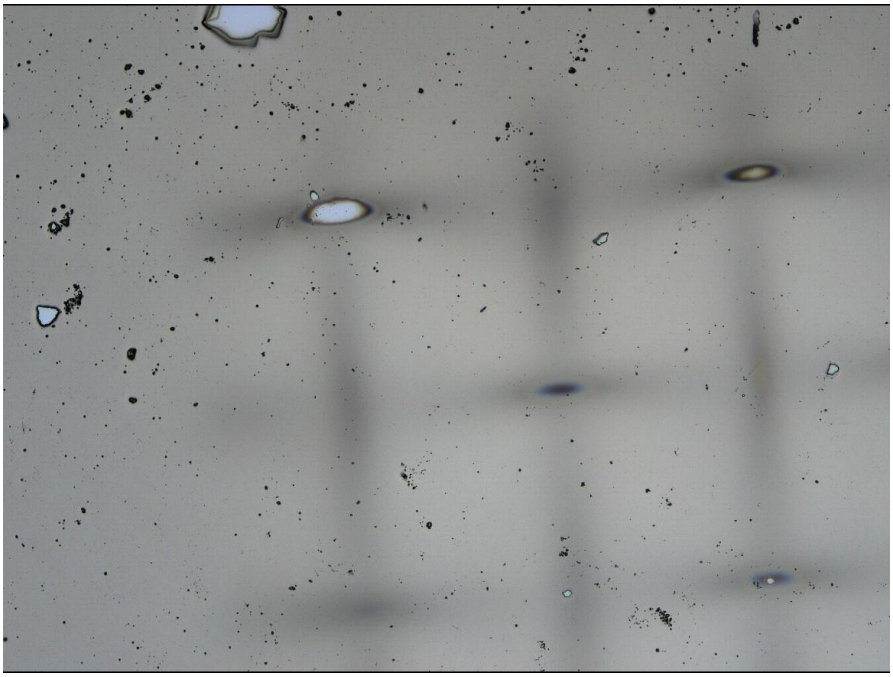

Figure 14: Deposition observed within the mesh grid area (1 mm scale bar)

As for the other four specimens, results were analyzed in terms of both thickness (*Fig. 15*) and volume (*Fig. 16*). It was observed that thickness differences were particularly marked compared to volumetric ones, since the latter also accounted for the enlargement of the deposition radius: the deposited layer extended over a larger area, thus further reducing the average thickness.

A key aspect of this analysis was the introduction of a threshold thickness value, defined as the “target thickness.” This parameter represents the minimum limit required to ensure the reliability of subsequent SEM and nanoindentation investigations, avoiding the influence of the silicon substrate on the results. This value was set at 2 µm, considered sufficient to maintain a film layer at least ten times thicker than the expected indentation depth (~200 nm), and thick enough to prevent SEM electrons from penetrating through the layer during analysis. This choice thus ensured the validity and significance of the mechanical and structural analyses later conducted on the samples.

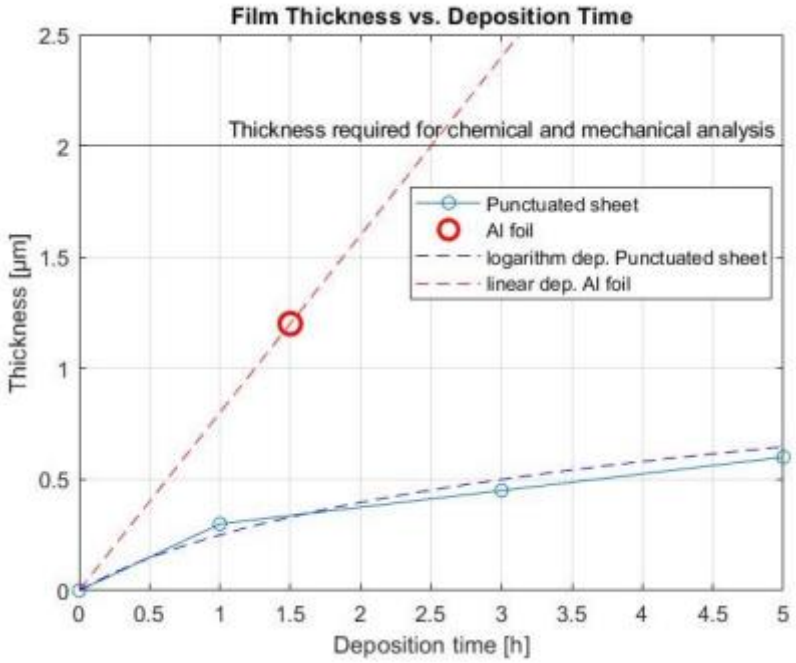

Figure 15: Differences in deposition thickness

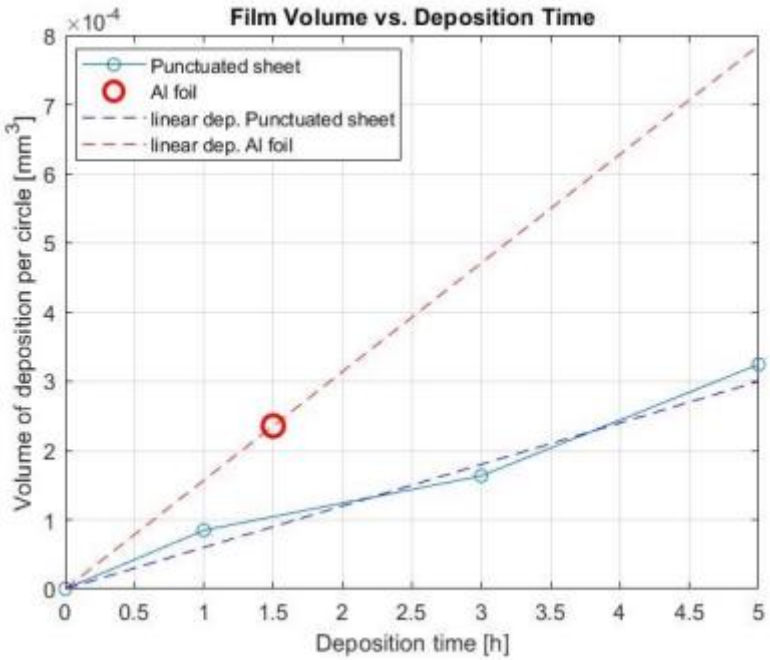

Figure 16: Differences in deposition volume

From the obtained results, it became clear that using the punctuated sheet led to extremely long deposition times, on the order of several days, to reach the established target thickness. Conversely, the use of a simple aluminum foil allowed the same result to be achieved in about 2.5 hours. The difference is therefore substantial and plays a crucial role not only in time management but also in optimizing the entire experimental process.

Deposition time is not a secondary parameter: it directly determines how quickly subsequent analyses can be performed and is proportional to the amount of target material consumed. This has not only economic implications but also practical ones, since target replacement requires inevitable interruptions. Considering that targets, with thicknesses between 1 and 6 mm, must be replaced every 12–20 hours of use, adopting solutions that dramatically increase deposition times introduces a significant burden on specimen production. This makes the entire workflow inefficient and hinders the smooth progress of analyses, highlighting how the choice of coverage type represents a determining factor for the success of the project.

2.4 Deposition System for Thin Films

The deposition of thin films requires careful selection of the experimental configuration, as the chosen parameters directly influence the quality of the coating and the

reproducibility of the results. In the initial phase of the work, it was therefore necessary to analyze the main PVD techniques available, identify the most suitable configuration, and evaluate possible support tools to ensure uniformity and compositional control of the deposited film. The choices made in this preliminary phase significantly influenced the subsequent steps, both from an operational and scientific perspective.

2.4.1 General Description of the System

The deposition system used for the fabrication of thin films consists of a high-isolation vacuum chamber, designed to simultaneously host multiple sputtering sources. The chamber, made of stainless steel, is equipped with optical windows and numerous flanges that allow the introduction of process gases and the accommodation of measurement and control lines. The vacuum required for the process is ensured by a two-stage pumping system: a preliminary rotary pump and a high-efficiency turbomolecular pump. The combination of these two devices allows achieving base pressures on the order of 10^{-3} Pa, an essential condition to minimize residual contamination and guarantee a controlled environment during deposition.

2.4.2 Deposition Sources: Multi-Target Magnetron

The chamber is equipped with a magnetron sputtering system configured for multi-target operation. This allows the simultaneous or sequential deposition of different materials by appropriately varying the power applied to each target. The magnetrons are water-cooled to maintain stable target temperatures and prevent deformations or uncontrolled variations in the flux of ejected atoms.

2.4.3 Main Operating Parameters: Target–Substrate Distance, Power, Pressure

Target–Substrate Distance

In [25], an algorithm was studied to determine the deposition conditions of the films. Parameters such as the target material, the target–substrate distance, the vacuum level, the sputtering power, etc., were considered, and an approach was organized to explore these parameters systematically.

Initially, when a magnetron sputtering source is positioned in front of the substrate at a distance L, the ratio between the sputtering radius of the magnetron R and the distance L is defined as $x_1 = R/L$, and the ratio between the distance from the substrate center x and the distance L as $x_2 = x/L$. The deposition rate D(x) at position x can be approximately expressed as:

$$D(x) \propto \frac{1}{\left(1 + \left(\frac{x}{L}\right)^2\right)^{3/2}}$$

x = distance from the substrate center

L = target–substrate distance

the exponent 3/2 derives from the assumption of emission following the cosine law

This function, when x_1 = R/L is sufficiently small, becomes a monotonically convex curve; moreover, differences in deposition rate as a function of position x on the substrate are reduced. Since our magnetron sputtering is designed with R = 20 mm (as used in the laboratory), it is necessary to preselect an appropriate distance L.

In our experimental setup, the chosen target–substrate distance is L = 121.5 mm. This value represents an optimal compromise: on one hand, it maintains a sufficiently uniform deposition profile on the specimen, reducing local variations in the film growth rate; on the other, it ensures that the particle flux from the target is not excessively dispersed. Considering that the typical sample size is approximately 1.5 cm, analysis of D(x) shows that within ±7.5 mm from the center, the deposition rate variation remains within a narrow range, below about 10% relative to the average value, thus ensuring high coating uniformity.

It is important to emphasize that some variation in the deposition rate is advantageous: very small values of L would produce excessive variation, compromising film uniformity, while very large values would create an almost flat distribution, losing the degree of freedom needed to study different material percentages within the same specimen. This compositional gradient along the surface is crucial to explore different mixtures and identify promising compositions efficiently. Furthermore, L cannot be reduced arbitrarily: introducing multiple targets requires sufficient space to avoid undesired overlap of atomic fluxes and maintain an adequate vacuum level. Therefore, the adopted value of 121.5 mm represents a balance between film uniformity, process efficiency, and the possibility of achieving useful compositional gradients.

Power

Regarding the sputtering power, the sputtering efficiency at 0.5 keV (i.e., the ratio between incident ionized gas atoms and atoms emitted from the target) is well-known. For the elements of interest, the values are reported in Table 1. Even if some elements have not yet been studied, it is possible to build a database with these data and define

basic conditions for alloy formation. In magnetron sputtering, the number of incident ions generally corresponds to the current supplied; thus, the amount of material emitted from the target can be assumed as the product of current and sputtering rate. By analyzing process data with the known sputtering rate, it is possible to estimate system parameters independently of the material.

Target	Sputtering rate
Al	1.05
Cu	2.35
Ni	1.45
Ti	0.51
V	1.05
W	0.57
Zn	1.85

Table 1: Sputtering rates with argon ions at 0.5 keV (atoms/ion)

It can be noted that the table does not report the sputtering ratios for all the elements used. This prevents a priori prediction of the deposition rate. Conversely, once the deposition rate has been measured, deductions regarding the individual sputtering ratios can be made.

The adjustment of power can be performed by controlling either the current or the voltage, given the overall system resistance. In this work, current control was selected, as it is directly proportional to sputtering frequency and thus more representative of the deposition process. Experimentally, voltage is observed to vary depending on the selected current, the target material, and its usage time. In particular, as the target erodes, the voltage tends to decrease due to the surface geometry changes, which facilitate the sputtering process and effectively reduce the system's electrical resistance.

Pressure

An equally important role is played by the internal chamber pressure, which directly influences the likelihood of collisions between ejected particles and the medium (mainly argon, plus air and impurities), determining the microstructural quality and final composition of the deposited film. Here again, pressure selection represents a compromise: high pressures favor scattering of sputtered atoms inside the chamber, compromising directionality and uniformity; conversely, very low pressures make

plasma creation and stabilization difficult, requiring progressively higher electrical power as the pressure decreases.

2.5 Film Production

2.5.1 Definition of Film Compositions

The experimental activity was organized progressively, aiming first to understand the fundamental characteristics of the single elements and then to proceed to the fabrication of multicomponent films. As a first step, the deposition rate was studied, a key parameter for system calibration, and for the subsequent definition of target compositions. For each selected element, three distinct specimens were produced, varying the deposition time at 0.5, 1, and 2 hours, respectively. A linear trend of film thickness versus deposition time was expected, allowing a quantitative estimate of the growth rate (Fig. 19).

The elements chosen for this preliminary phase were TiAl, Zr, Hf, and V. Their selection was motivated by three main factors: (i) their recognized use in the nuclear industry, making them relevant from an application standpoint; (ii) the immediate availability of targets in the laboratory; and (iii) the scientific interest in exploring relatively unstudied but promising combinations for forming cohesive and robust films on silicon substrates. Moreover, compatibility among these elements suggests the possibility of obtaining thin alloys with favorable mechanical and structural properties.

Once the single elements were characterized, multicomponent films were deposited using two main configurations of the multi-target system. In the first configuration, the targets Zr, Hf, and TiAl were employed; in the second, V, Hf, and TiAl were used. In each configuration, specimens containing all possible binary combinations were produced to systematically investigate the properties resulting from the interaction of element pairs. Finally, a ternary film including all three elements was fabricated for each configuration, aiming to assess the formation of high-entropy structures and evaluate the stability and uniformity of the resulting deposition.

This structured workflow allowed the experimental process to proceed in progressive and complementary phases: from characterizing the deposition rates of individual targets to testing pairwise behavior, and finally to fabricating more complex multicomponent films, thus providing a solid foundation for the detailed analyses discussed in the following chapters.

2.5.2 Data Recording and Deposition Monitoring

During each deposition, operational parameters and process conditions were systematically recorded to ensure full traceability of the produced specimens. Continuous monitoring included chamber pressure, the current and voltage applied to the magnetrons, total absorbed power, and the temperature of the cooling supports. Additionally, optical inspection of the plasma was conducted at regular intervals to verify stability and prevent abnormal discharge events. The collected data serve as a fundamental reference to correlate process conditions with the final film properties and to identify any undesired deviations.

2.5.3 Reproducibility and Standardization Strategies

A central aspect of the work was the development of strategies to ensure the reproducibility and standardization of the samples. Strictly controlled preparation and deposition procedures were defined, including preliminary chamber cleaning steps. Each deposition sequence was repeated multiple times under nominally identical conditions to evaluate the intrinsic variability of the process. Every step, from sample preparation to deposition, was executed with careful attention to minimize external factors that could compromise film quality.

Moreover, all significant data for each specimen were meticulously recorded; the main values are summarized in Appendix A, providing a clear and comparable reference for the entire set of produced samples.

This approach extends beyond experimental purposes: the ultimate goal of the study is to define industrial recipes that can be faithfully replicated at a production scale. Ensuring full reproducibility of the samples is therefore crucial, as it represents the necessary condition for transferring laboratory results to real industrial processes, guaranteeing the desired material quality and properties on a larger scale.

2.5.4 Maintenance of the PVD Deposition System

The PVD deposition system used in this work, designed by Professor Murakami, was conceived with the goal of being cost-effective while enabling rapid sample production. However, during the research period, it became evident that maintenance represents one of the most critical aspects for the operational efficiency of the system, as it constitutes the main cause of time loss.

Maintenance of the PVD system is necessary for several reasons. Firstly, failures can occur in essential subsystems, such as one of the two installed vacuum pumps, the

water-cooling circuit for the targets, or the power supplies required to generate the plasma. Timely detection and resolution of these issues are crucial to minimize downtime and ensure continuity of the deposition process.

During normal operation, the deposition chamber inevitably becomes contaminated. This requires periodic cleaning, which involves opening the chamber, removing the components to be cleaned, and performing manual or chemical cleaning procedures. In this research, manual cleaning was the primary approach: larger metallic surfaces were cleaned by hand, while smaller components were immersed in an acetone solution. The solution effectively removes adhered impurities, allowing for a thorough and safe cleaning of delicate parts.

Another critical aspect of maintenance concerns the periodic replacement of targets, which are consumed during deposition. This operation requires particular care, as the targets and surrounding walls must be electrically insulated to create the potential difference necessary for plasma formation. The placement of the targets is therefore critical: it is necessary to carefully measure the ohmic resistance at multiple points in the deposition gun to ensure it is not zero and to verify proper electrical separation between components.

In summary, maintenance of the PVD system is central to ensuring both the continuity and quality of the depositions. Proper management of all subsystems, pumps, cooling, power supply, chamber cleaning, and target replacement, allows for minimizing downtime, optimizing process efficiency, and ensuring reproducibility of the produced samples, a fundamental objective for the scientific research conducted in Professor Murakami’s laboratory.

Figure 17: details of the machine during maintenance

In Figure 17, the upper part of the machine can be seen, including the three cannons and the plastic tubes used to circulate the coolant. Only the upper section requires the use of argon to lift it, as it is very heavy. Additionally, all removable parts rely on bolts that must be screwed and unscrewed each time the chamber is opened. A detail of the three loaded targets is also shown on the right. As can be seen, the targets (originally perfect discs) are worn. In particular, a circular erosion is visible, which can eventually perforate the entire target if it is not replaced.

2.6 Analysis of Single-Component Films

2.6.1 Objective of Single-Component Film Analysis

The initial depositions were dedicated to the production of single-component films, with the aim of determining the deposition rate of each element. This preliminary analysis is essential, as it is not possible to directly measure the contribution of each individual element during simultaneous deposition from multiple targets. Knowledge of the deposition rate of single elements also allows precise prediction of the component percentages in multicomponent specimens, facilitating control of compositional gradients and obtaining films with desired characteristics.

For each selected element (TiAl, Zr, Hf, and V), three specimens were prepared with deposition durations of 0.5, 1, and 2 hours. Measurements obtained through optical profilometry confirmed an approximately linear relationship between film thickness and deposition time, providing a quantitative foundation for designing multicomponent films. At this stage, chemical composition was not taken into account, as single-element deposition is expected to yield a uniform distribution.

2.6.2 Case of Zinc: Limitations Due to Boiling Temperature

An attempt was also made with zinc to evaluate its compatibility with the sputtering process. However, this experiment proved unsuccessful. Zinc's relatively low boiling temperature resulted in extremely widespread deposition, with material spreading throughout the chamber (Fig. 18). This phenomenon led to the formation of a zinc layer on all internal surfaces, including other targets, requiring careful disassembly and cleaning of the entire system. In particular, deposition on other targets caused issues in subsequent depositions; the ideal conditions were reached only after removal and thorough cleaning of the additional targets. This experience demonstrated that the use of elements with low boiling points can compromise both film quality and operational efficiency, causing significant delays. Consequently, zinc was excluded from future depositions, focusing exclusively on elements with high boiling points, which are more suitable for accurate deposition control and reproducibility of specimens.

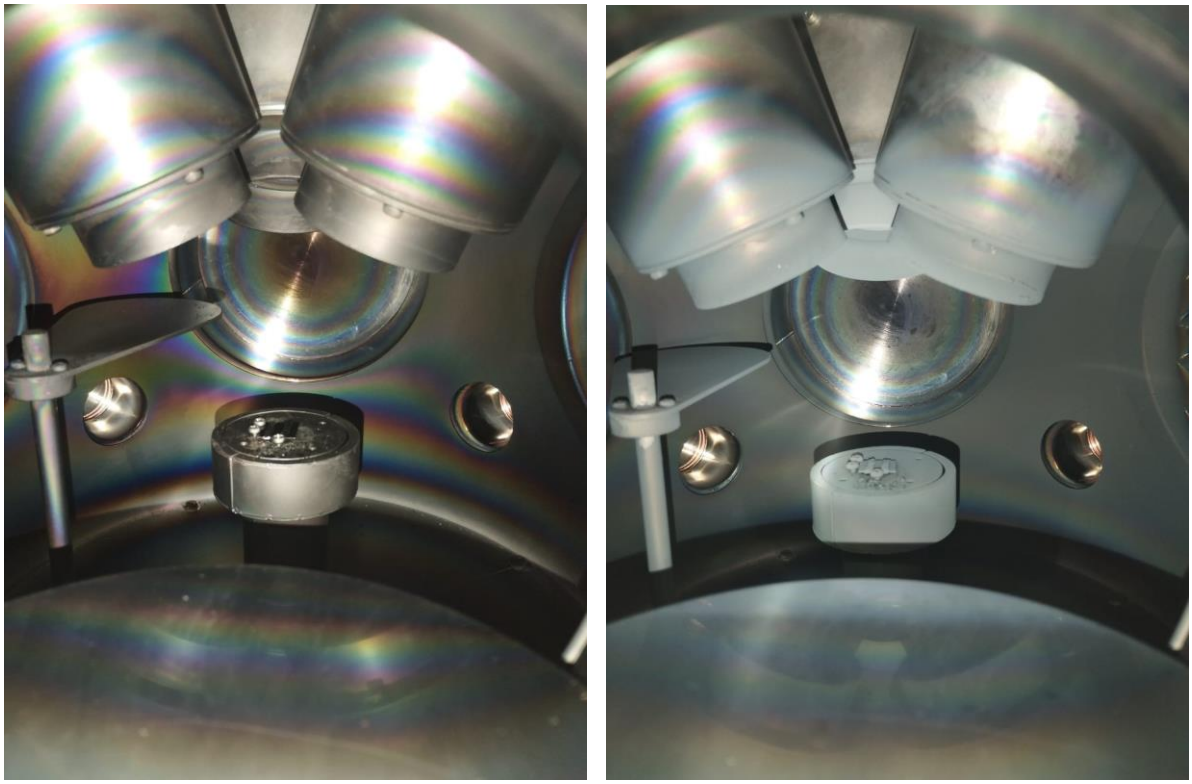

Figure 18: chamber before and after zinc deposition

2.6.3 Deposition Rate Trends

To complete the preliminary analysis of single-component films, graphs representing the thickness versus deposition time for each element were produced. These data allow comparison of the deposition rates of different materials and identification of which targets contribute most rapidly to film growth (Fig. 19).

Experimental results clearly indicate that V and TiAl are the slowest-depositing materials, while Zr and especially Hf show significantly higher deposition rates. This behavior can be directly correlated with the specific sputtering rates of each element, determined by the combination of the target's physical properties and the operational conditions of the magnetrons.

The values reported in the graphs represent averages: for each specimen, 16 measurements were taken across the surface, and the final value was calculated as the arithmetic mean of these readings. It is important to note that film thickness varies with distance from the target; therefore, deposition is not uniform across the entire surface. Additionally, measurements can only be performed in the transition zone between the uncoated area (protected by the aluminum foil) and the deposited area; consequently, direct information on the film thickness in most of the specimen surface is not available. However, the measured values are considered sufficient to reasonably estimate the thickness in the unmeasured regions.

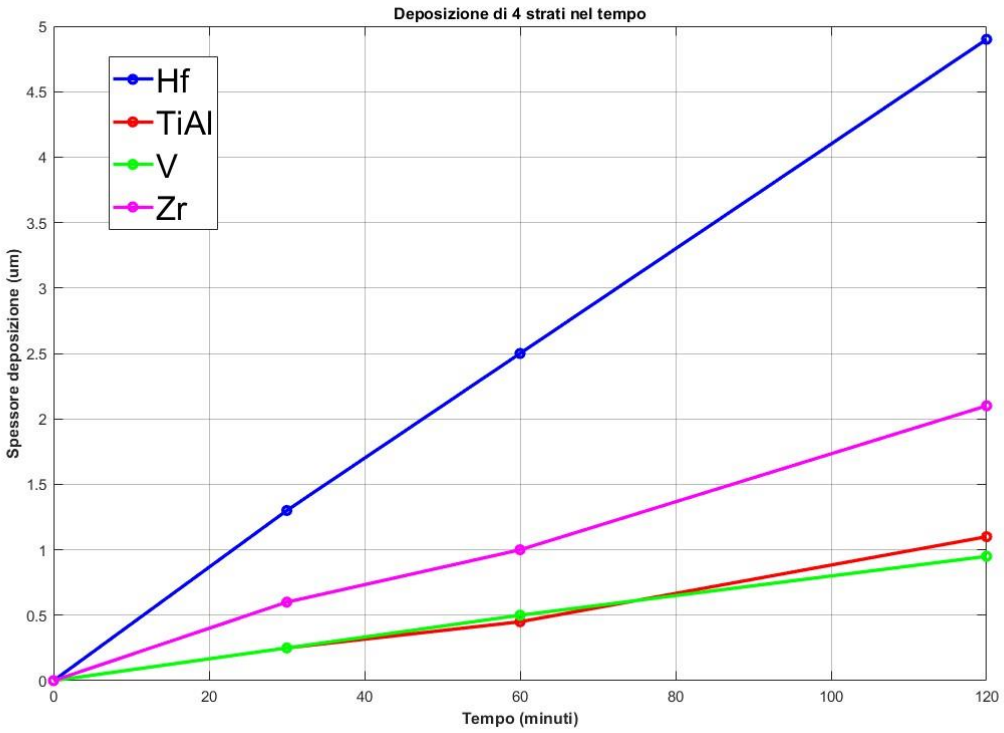

Figure 19: Film thickness trends over time

2.6.4 Case of Zirconium

During Zr single-component depositions, the film was observed to adhere poorly to the silicon substrate. Alcohol treatments revealed pronounced peeling, suggesting a possible chemical-physical incompatibility between Zr and the substrate.

To improve adhesion, a preliminary TiAl deposition of approximately 10 minutes was implemented, followed by the actual Zr deposition. This strategy created an intermediate layer that promotes film anchoring, enhancing cohesion.

The results showed a significant improvement in film stability, as evidenced in Figure 20, where the separation observed in the initial depositions is compared with the greater resistance achieved after using the TiAl intermediate layer.

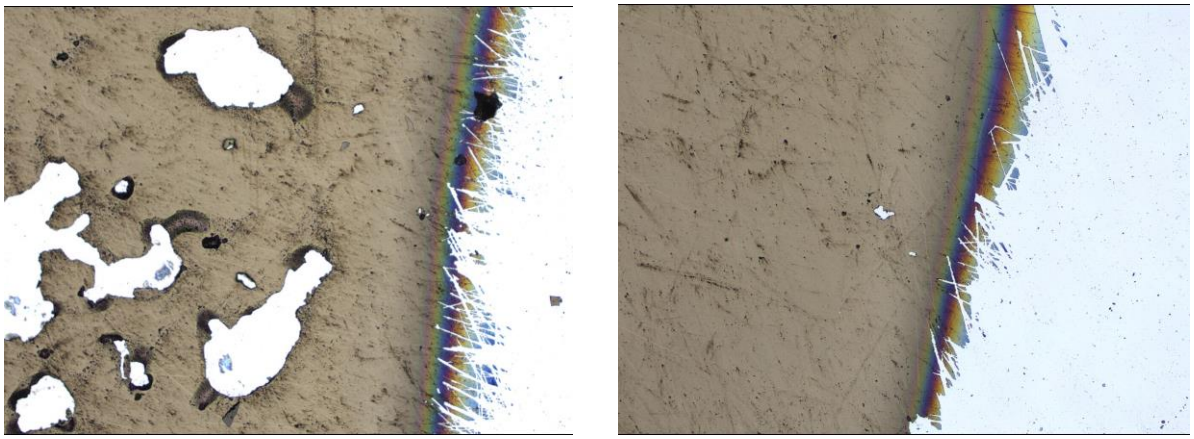

Figure 20: alcohol treatment without and with initial TiAl layer (100 µm scale bar)

2.7 Analysis of Multicomponent Films

After the preliminary phase dedicated to single-component films, the study focused on the production and characterization of multicomponent specimens, with the aim of evaluating not only the deposition rate of the different elements but also the mechanical, chemical, and structural properties of the resulting films. Unlike the initial experiments, which were mainly exploratory and aimed at calibration, this phase required the use of advanced analytical tools capable of providing quantitative and high-resolution information.

Investigations were carried out using nanoindentation to characterize local mechanical properties of the films and scanning electron microscopy (SEM) to analyze surface morphology and microstructure. Energy-dispersive X-ray spectroscopy (EDS) was employed to determine the elemental chemical composition of the films and to construct two-dimensional maps of element distribution. In parallel, film thickness measurements were still performed using optical microscopy, providing information on deposition uniformity and verifying potential gradients across the surface, ensuring that the measured thickness corresponded to the expected sum of the individual elements' contributions.

The combination of these techniques allowed a comprehensive understanding of the behavior of multicomponent films, integrating structural, chemical, and mechanical data. The analysis enabled two-dimensional visualization of the entire 15 × 15 mm specimen surface, allowing a more accurate representation of compositional inhomogeneities. The approach in this phase was therefore more structured and methodical, as the goal was no longer only to determine deposition rates, but also to validate a predictive method capable of accurately reproducing the final film composition based on process parameters.

2.7.1 Surface Morphology

This section presents selected SEM images of the surface of several specimens. Thanks to the high resolution of the JSM-7001F scanning electron microscope, nanometric details of the surfaces can be clearly distinguished, providing precise insight into the microstructural features of the deposited films.

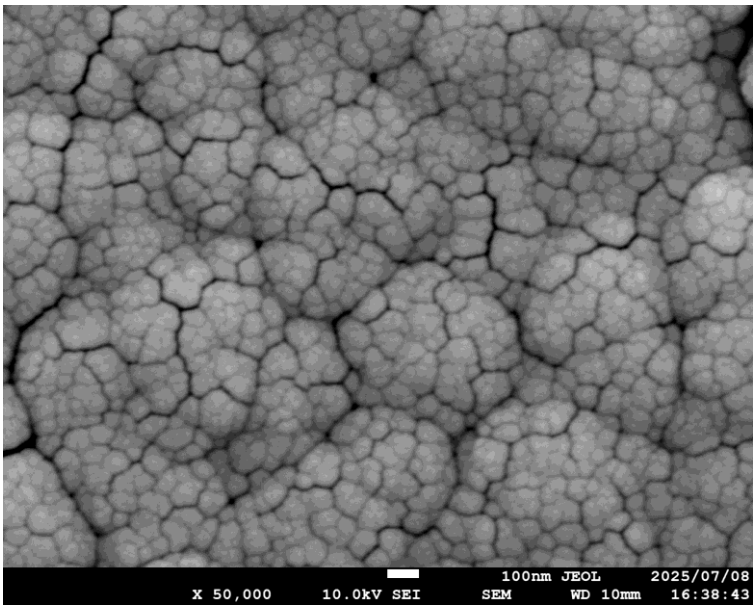

Figure 21: example picture of specimen 20250708-1 surface (100 nm scale bar)

The images reveal well-defined grain boundaries and cracks propagation (Fig.21), allowing for the identification of individual grains and the evaluation of surface quality. The clarity of these boundaries is particularly useful for assessing the uniformity of the coating and detecting possible defects, irregularities, or discontinuities that could affect the functional performance of the material.

In the case of zirconium-based specimens, crystalline formations are clearly visible on the surface (Fig. 22). Moreover, one specimen displayed extreme variations in surface morphology across different areas, highlighting the heterogeneity that can arise even within a single deposition. These observations underscore the importance of high-resolution imaging in evaluating both the microstructural characteristics and the overall quality of thin-film surfaces.

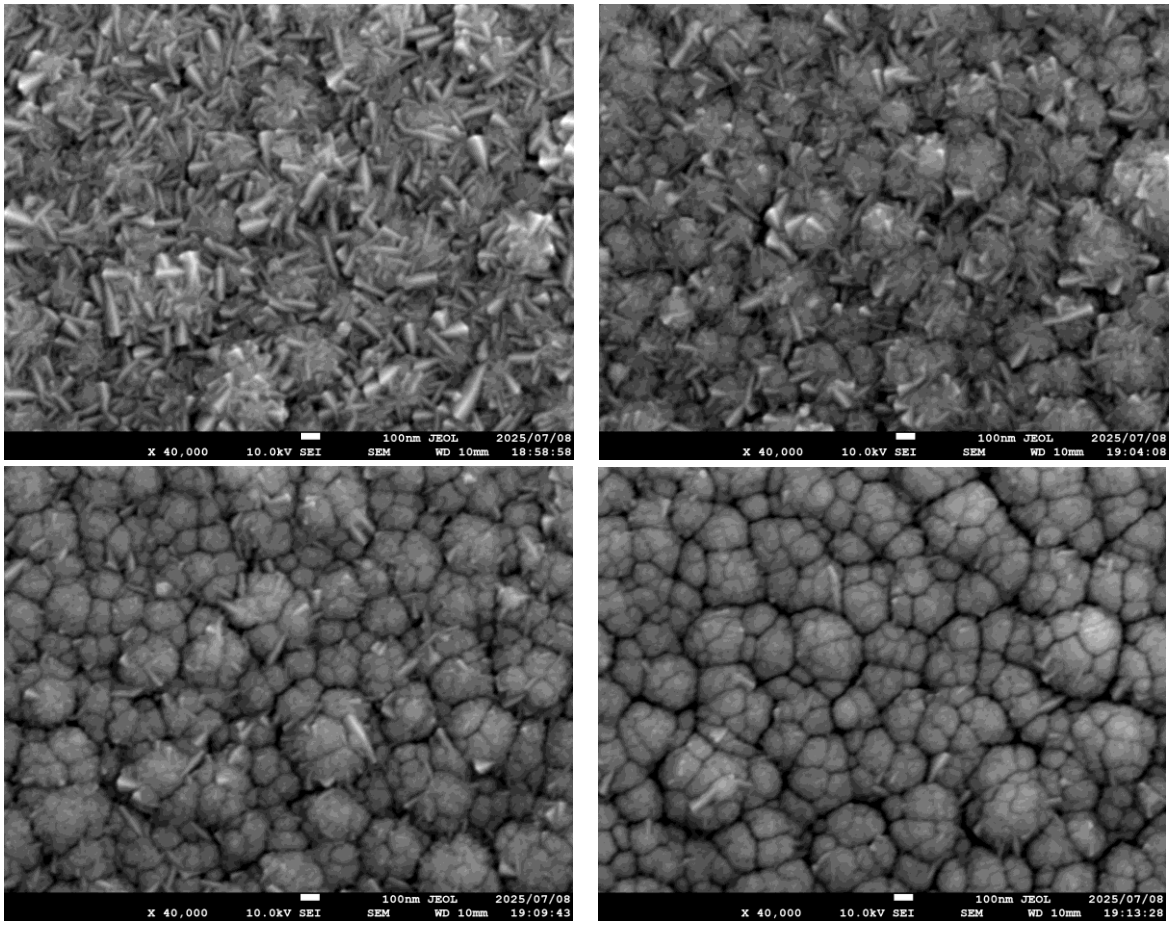

Figure 22: Surfaces of specimen 20250630-2 with decreasing Zr% (100 nm scale bar)

2.7.2 Elemental Distribution

EDS maps acquired on multicomponent specimens allowed visualization of the chemical distribution in two dimensions and comparison of measurements with predictions based on deposition parameters. The first aspect observed is the variation of composition with distance from the targets. As expected from theory and confirmed by literature studies, the percentage of each element in the film gradually decreases with increasing distance from its corresponding target. This behavior indicates that the spatial distribution of elements follows a law consistent with sputtering physics and the deposition solid angle.

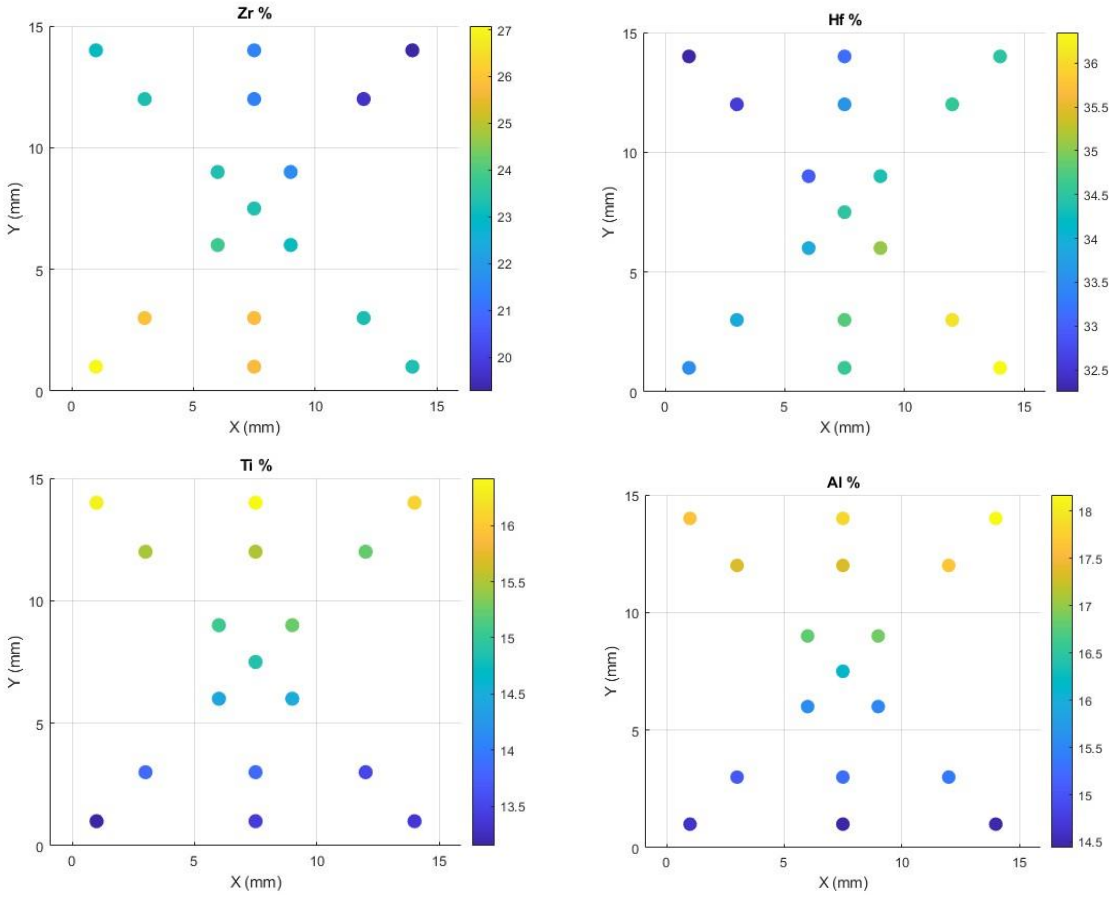

Figures 23: Chemical composition of the ternary HfZrTiAl specimen

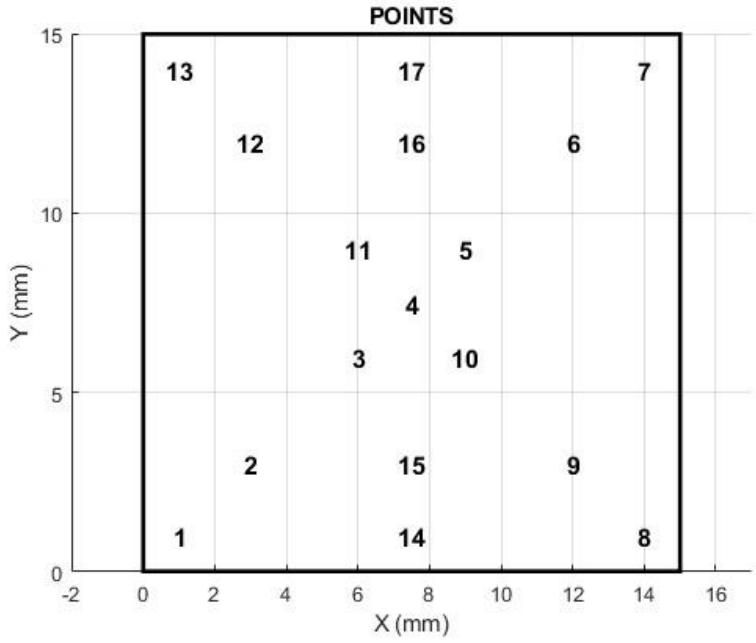

Figure 24: Locations of measurement points on the specimen

2.7.3 Comparison with Theoretical Predictions

The thicknesses of specimens consisting of two elements were compared to verify the relationship between the contributions of the individual constituents and the overall film thickness. Analysis showed that the sum of the thicknesses attributable to individual elements closely reproduces the final observed thickness, confirming the consistency of the deposition process with the expected additive model (Table 2). As an example, results for two binary specimens are reported: the first composed of TiAl–Zr and the second of Hf–V, for which agreement between theoretical and experimental values was observed.

Specimen	Expected dep Element A [µm]	Expected dep Element B [µm]	Theoretical Total [µm]	Measured Thickness [µm]
TiAl–Zr	0.45	1.05	1.50	1.40
Hf-V	2.50	0.50	3.00	2.75

Table 2: Predicted deposition rates for binary specimens

It should be noted that both specimens were produced maintaining a constant current of 0.5 A and a deposition time of one hour; therefore, the deposition rate is expected to be consistent with that reported in Fig. 19. As observed, the deviation between theoretical and measured thickness is below 10% in both cases, confirming the reliability of the process. However, it is important to highlight that the first specimen has a total thickness below 2 µm, considered the minimum value to ensure meaningful results from EDS analysis. For this reason, this sample was not used in subsequent investigations, and the corresponding chemical composition maps are not reported.

2.7.4 Mechanical properties

Finally, the mechanical properties of the deposited films are presented. In particular, the Young's modulus and Poisson's ratio were evaluated for various specimens. To ensure the reliability and accuracy of the collected data, each point on the surface of every specimen was measured five times, and this process was repeated across nine different regions of the specimen.

This procedure of performing multiple measurements around the same point is necessary because the surface may present local imperfections (Fig. 25) that could lead to significant errors if only a single indentation were performed. By slightly shifting the indenter by a few micrometers and performing multiple indentations over a very small area (Fig.26), it is assumed that the intrinsic behavior of the material remains constant, allowing for the collection of more representative data.

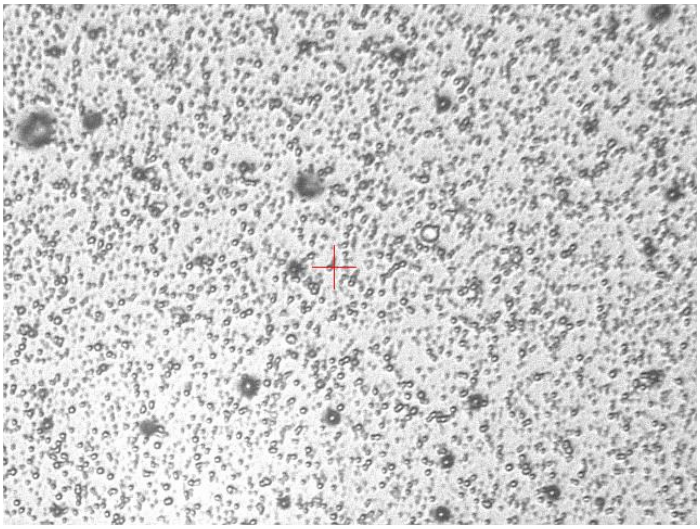

Figure 25: surface example with high presence of discontinuity (100 µm scale bar)

For each measured point, the arithmetic mean of the repeated measurements was calculated and considered as the final value. Subsequently, the instrument proceeded to measure all the other designated regions on the specimen. It is evident that this procedure requires a considerable amount of time. Considering an average of 2 minutes per indentation and a total of 45 indentations per specimen (9 regions × 5 measurements), each specimen required at least 90 minutes of measurement time. This not only represents a significant investment of researchers' time but also constitutes a repetitive and labor-intensive task.

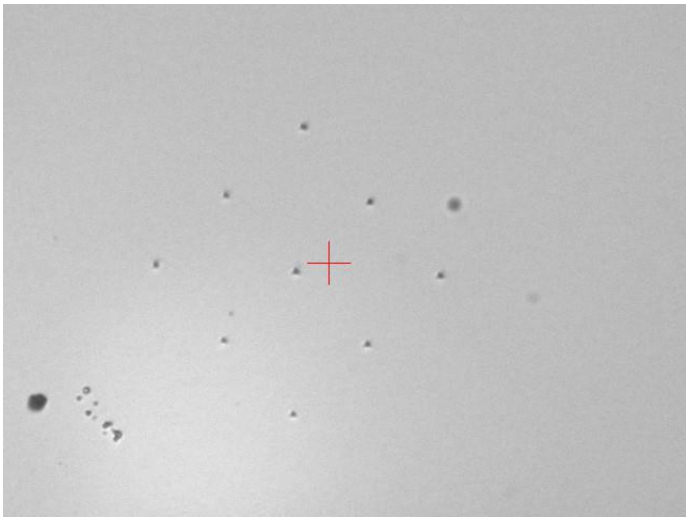

Figure 26: Example of 9 indentations carried out around one measurement point (100 µm scale bar)

Furthermore, it should be noted that for industrial applications, an even higher number of indentations per region is typically required, sometimes up to 20 measurements per

zone, to obtain statistically meaningful results. This highlights the absolute necessity of automated indentation systems, which allow both a significant reduction in measurement time and an increase in data reliability, while minimizing the physical strain on operators.

Finally, a graph is reported for six measurements acquired at the second point of specimen 20250708-1. In this graph, the y-axis represents the applied load, while the x-axis indicates the penetration depth. The shape of the load–displacement curve itself is an indicator of the quality of the measurement: large discontinuities or irregularities in the curve suggest that something went wrong during the test, either due to surface inhomogeneity at the selected point or because the applied load was not properly chosen. In the present case, the obtained curves are considered acceptable and representative of reliable measurements.

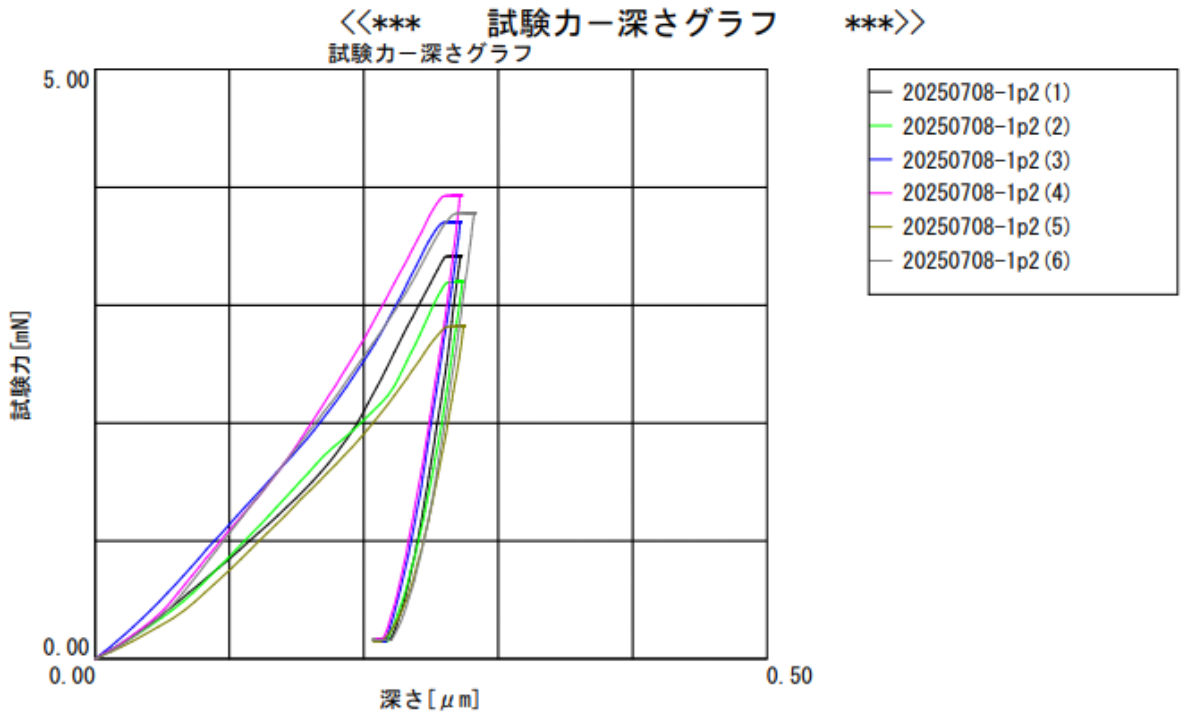

Figure 27: load–displacement graph for 6 measures of point 2 of 20250708-1 specimen

Table 3 summarizes the mechanical properties obtained from the indentation tests, namely the Indentation Modulus (E_it) and the Indentation Hardness (H_it), expressed in N/mm^2.

The Indentation Modulus represents the elastic response of the material under localized loading. It is derived from the slope of the unloading portion of the load–displacement curve according to the Oliver–Pharr method and is closely related to the

Young's modulus of the specimen. This parameter provides valuable information on the stiffness of the deposited films.

The Indentation Hardness, on the other hand, reflects the resistance of the material to plastic deformation under the applied load. It is calculated as the ratio between the maximum applied load and the projected contact area of the indentation. Higher hardness values indicate a stronger resistance of the film surface against permanent deformation.

Together, these two parameters give a comprehensive picture of the mechanical behavior of the deposited films, enabling a direct comparison between the analyzed specimens in terms of both elastic and plastic response.

specimen	Maximum Force [mN]	penetration height [µm]	E_it [N/mm^2]	H_it [N/mm^2]
20250625-1	5.10	0.235	1.007e+05	4017
20250627-1	7.53	0.189	1.113e+05	6220
20250630-1	6.50	0.198	1.054e+05	5139
20250630-2	6.45	0.207	1.060e+05	3649
20250707-2	4.59	0.210	9.915e+04	3625
20250708-1	3.72	0.231	6.070e+04	2670
20250708-2	8.11	0.182	1.146e+05	7353
20250709-1	10.3	0.147	1.139e+05	10070

Table 3: Mechanical properties of the analyzed specimens

2.8 General Conclusions

The research presented in this thesis systematically addressed the study, deposition, and preliminary characterization of multicomponent thin films on silicon substrates, with the aim of developing innovative materials for nuclear applications. The approach followed allowed for a comprehensive understanding not only of deposition techniques and their critical aspects, but also of the analytical methods necessary to ensure reproducibility, control, and validation of the results obtained.

The first part of the work focused on the preliminary deposition phases, with particular attention to single-component specimens. This methodological choice was crucial for determining the deposition rate of each element, a parameter not directly measurable during simultaneous multi-element depositions. The measurements performed

allowed for reliable average values for each material to be established, providing a solid basis for quantitatively predicting the final composition of multicomponent films. In this phase, the specific case of zinc had to be addressed, as it proved unsuitable due to its low boiling point, which led to uncontrolled distribution of the material throughout the deposition chamber. This event required a critical review of the materials selection, leading to a focus exclusively on elements with higher boiling points and better stability characteristics.

Subsequently, analyses on multicomponent specimens represented a crucial step toward the study of complex coatings potentially applicable to engineering systems. In this phase, a more in-depth characterization was introduced, using advanced tools such as SEM and nanoindentation, complemented by optical measurements and EDS analysis. The data collected highlighted two fundamental aspects: on one hand, the variation of chemical composition with distance from the respective target, in agreement with theoretical models and available literature; on the other hand, the ability to quantitatively predict the ratios between different elements based on current intensity and deposition time. This result demonstrates that, through a systematic approach, it is possible to build reliable predictive models for the fabrication of multicomponent films.

Comparisons between depositions performed with and without grids allowed further operational conclusions to be drawn. Depositions with grids ensured greater compositional uniformity and higher reproducibility, albeit with a reduced deposition rate. Depositions without grids, on the other hand, showed an increased rate but with lower uniformity. The final choice to proceed favoring the configuration with grids was therefore dictated by the need to maintain maximum control over film quality, an essential condition for subsequent studies.

A particularly relevant outcome of the work was the improvement in the adhesion of zirconium films thanks to an interfacial treatment based on a preliminary TiAl layer. This solution resolved the initial adhesion problems observed in the first experiments with pure Zr, demonstrating the importance of carefully evaluating not only deposition parameters but also the compatibility between substrate and coating. This approach serves as a reference model for addressing similar issues in future studies on other materials.

Overall, the work laid the foundations for an integrated understanding of the deposition and characterization process of multicomponent films for nuclear applications. The methodologies developed and the data collected allow for a clear overview of the

potential and limitations of the employed techniques, while outlining possible pathways for future optimization.

It is important to emphasize that the results obtained in this thesis do not represent a definitive endpoint, but rather a fundamental step within a broader research effort. All the data collected will be integrated into a larger study conducted by the members of the Murakami Group, who will continue to gather similar data on other materials and on different combinations of the same elements. In parallel, further studies will be carried out in other laboratories at the University of Tokyo, where investigations will extend beyond structural, chemical, and mechanical properties to include the effects of ion and neutron irradiation.

These subsequent developments aim to test, under more realistic conditions, the resistance and stability of the deposited films, with the ultimate goal of assessing their potential applications in fission and fusion nuclear reactors. In this regard, this thesis has successfully established a solid methodological foundation, validated a reliable set of process parameters, and highlighted practical solutions for the deposition of complex films.

In conclusion, the work presented demonstrates how experimentation and predictive modeling can be combined for the development of new materials, paving the way for future research in which multicomponent alloys may play a central role in designing safer, more durable, and resilient nuclear systems. The contribution of this thesis should therefore be interpreted as an integral part of a larger research program, which will continue in the coming years and has the potential to yield tangible impacts in the field of materials engineering for nuclear energy.

APPENDIX A: Specimen deposition conditions report

Date	Start	End	P [Pa]	T [C]	V [V]	I [A]	Ar flow [cc/min]	Target
25/05/01	14:40	-	1.0	-	374	0.5	5	TiAl 70 30
-	-	16:40	0.96	-	359	0.5	5	-
25/07/07	14:10	-	21	22.2	330	0.5	25	TiAl 70 30
-	-	14:10	-	-	-	-	-	-
25/05/13	17:40	-	0.82	24.6	310	0.5	25	TiAl 70 30
-	-	20:40	0.81	37.8	294	0.5	25	-
25/05/20	13:15	-	0.84	26.1	298	0.5	25	TiAl 70 30
-	-	NP	0.81	34.3	NP	NP	25	-
25/05/27	16:54	-	1.55	25.7	392	0.5	25	TiAl 50 50
-	-	18:58	1.56	36.3	354	0.5	25	-
25/06/01	15:43	-	2.15	25.1	350	0.5	25	TiAl 50 50
-	-	17:43	2.15	34.4	328	0.5	25	-
25/06/02	19:31	-	1.85	27.8	345	0.5	25	TiAl 50 50
-	-	20:01	1.85	29.8	335	0.5	25	-
25/06/03	16:13	-	2.08	23.8	344	0.5	25	TiAl 50 50
-	-	17:13	2.08	30.5	320	0.5	25	-
25/06/10 -1	12:13	-	0.86	26.3	311	0.5	25	Zr
-	-	14:13	0.85	48.4	283	0.5	25	-
25/06/10 -2	16:09	-	1.83	29.3	245	0.5	25	Zr
-	-	17:13	1.83	39.1	-	0.5	25	-
25/06/17	18:29	-	1.6	26.1	286	0.5	25	Zr
-	-	18:59	1.55	33.6	248	0.5	25	-
25/06/18	17:08	-	1.50	24.6	250	0.5	25	Zr
-	-	19:08	1.50	42.1	230	0.5	25	-
25/06/19	14:28	-	1.50	25.4	235	0.5	25	Zr
-	-	15:28	1.50	36.3	224	0.5	25	-

25/06/19 -2	16:42	-	1.80	29.5	390	0.15	25	Zn
-	-	17;42	1.80	29.6	375	0.15	25	-
25/06/25 -1	13:30	-	1.7	27.2	319 254	0.5 0.5	25	TiAl 50 50 Zr
-	-	14:25	1.7	47.4	305 225	0.5 0.5	25	-
25/06/25 -2	15:30	-	1.55	34.8	238	0.5	25	Zr
-	-	16:25	1.55	42.1	222	0.5	25	-
25/06/25 -3	17:17	-	1.7	34.6	390	0.5	25	Hf
-	-	18:17	1.65	60.0	288	0.5	25	-
25/06/26 -1	14:45	-	1.7	24.7	294	0.5	25	Hf
-	-	16:45	1.7	64.4	274	0.5	25	-
25/06/26 -2	17:32	-	1.7	42.5	290	0.5	25	Hf
-	-	18:02	1.65	51.4	275	0.5	25	-
25/06/27	18:00	-	1.75	24.4	270 352	0.25 0.5	25	Hf TiAl 50 50
-	-	19:30	1.65	47.0	230 296	0.25 0.5	25	-
25/06/30 -1	14:45	-	1.65	25.6	266 230	0.5 0.5	25	Hf Zr
-	-	16:27	1.65	59.3	244 204	0.5 0.5	25	-
25/06/30 -2	17:19	-	1.62	35.1	225 197 319	0.2 0.3 0.5	25	Hf Zr TiAl 50 50
-	-	19:05	1.65	57.7	256 - 290	0.2 - 0.5	25	-
25/07/04 -1	15:24	-	2.10	24.2	340	0.4	25	V
-	-	16:27	2.10	29.8	311	0.4	25	-
25/07/04 -2	17:54	-	1.7	27.1	333	0.4	25	V
-	-	17:24	1.68	29.9	312	0.4	25	-
25/07/07 -1	14:10	-	2.00	24.6	330	0.4	25	V
-	-	16:10	2.00	32.6	291	0.4	25	-
25/07/07 -2	16:53	-	1.63	30.2	339 311	0.5 0.5	25	V TiAl 50 50

-	-	19:13	1.60	47.0	297 264	0.5 0.5	25	-
25/07/08 -1	14:30	-	1.62	36.2	243 313 275	0.25 0.5 0.5	25	Hf V TiAl 50 50
-	-	16:30	1.61	61.2	218 285 252	0.25 0.5 0.5	25	-
25/07/08 -2	18:00	-	1.62	250	246 313 278	0.3 0.5 0.5	25	Hf V TiAl 50 50
-	-	20:00	1.60	250	223 278 252	0.3 0.5 0.5	25	-
2025/07/ 09	16:40	18:40	1.72	31.7	248 307	0.4 0.5	25	Hf V
-	-	18:40	1.67	58.9	221 268	0.4 0.5	25	-

APPENDIX B: All specimen chemical maps

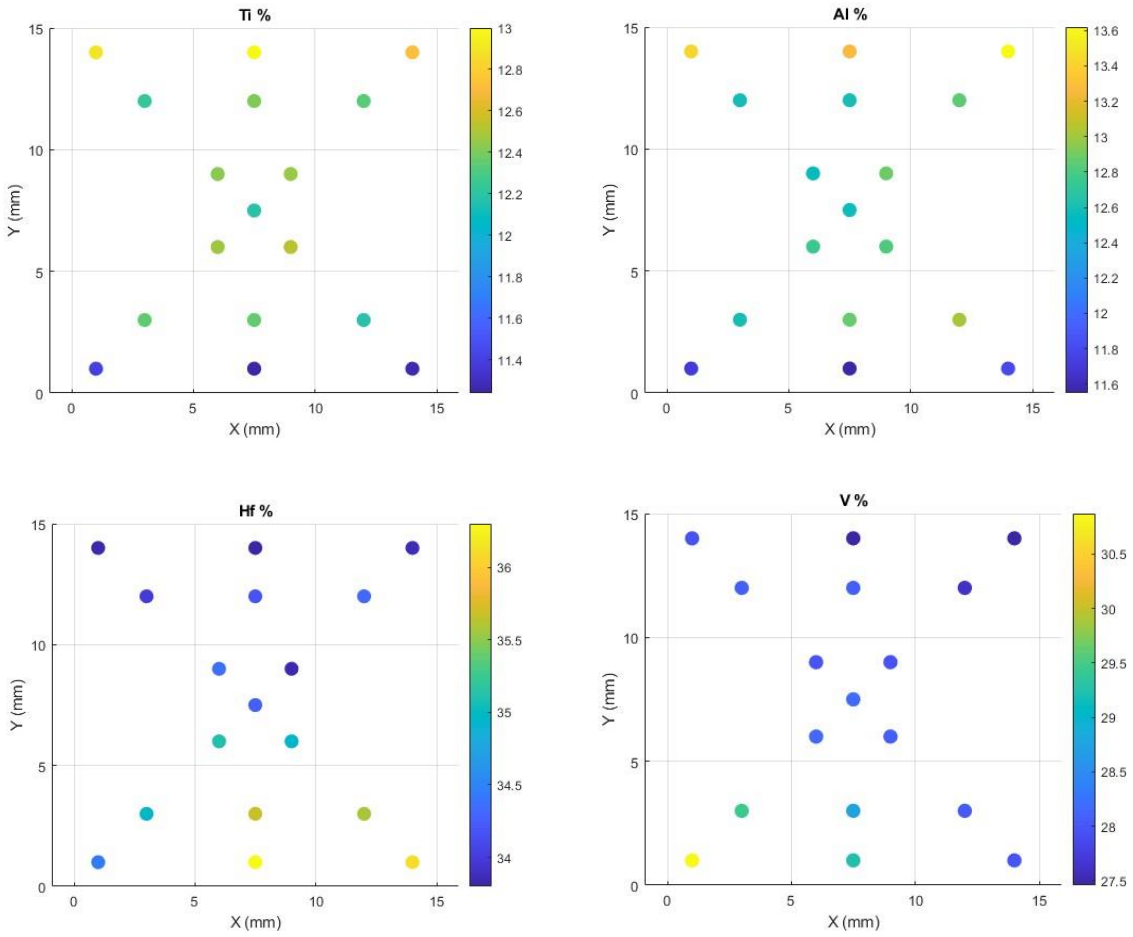

Figure B.1: Chemical maps of ternary HfVTiAl specimen

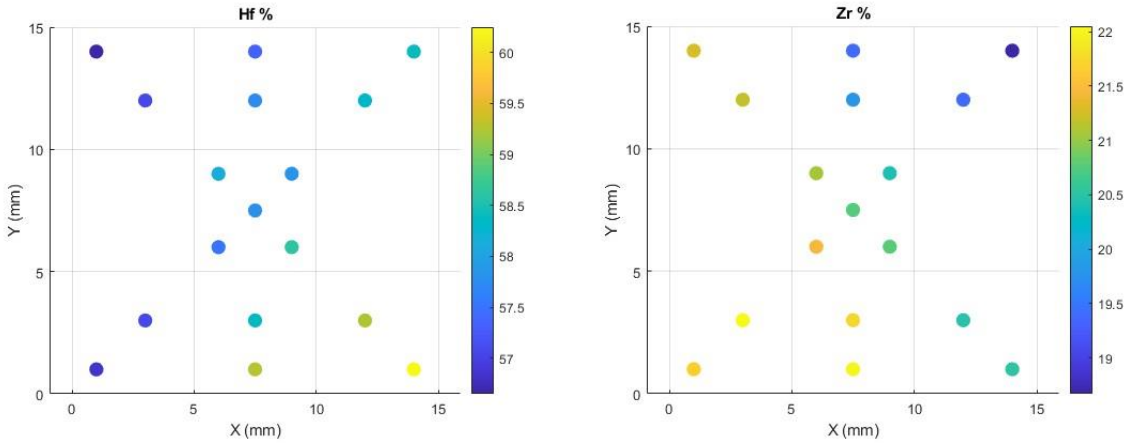

Figure B.2: chemical comp specimen ZrHf

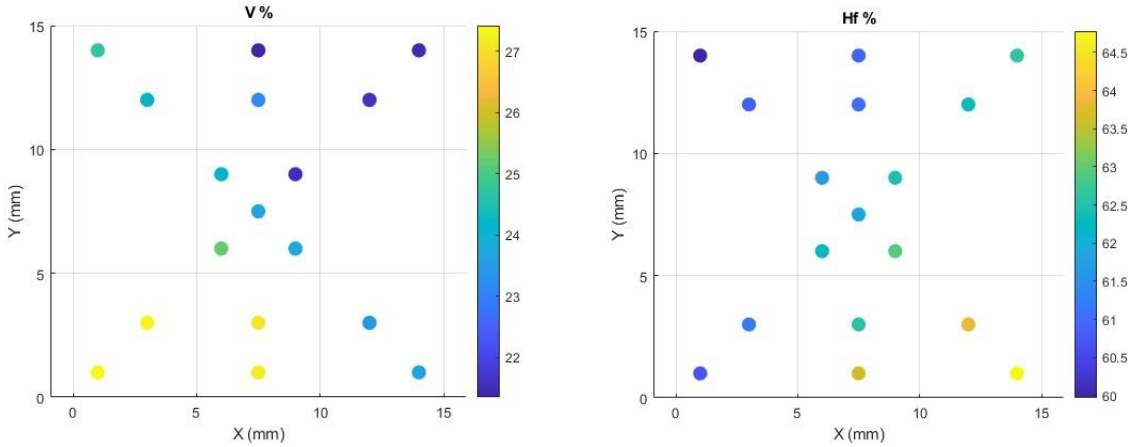

Figure B.3: chemical comp specimen HfV

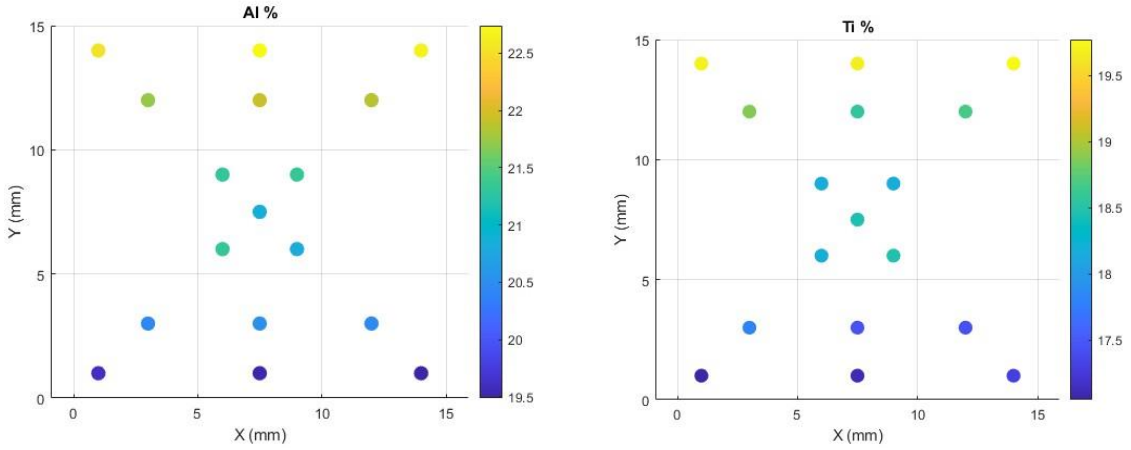

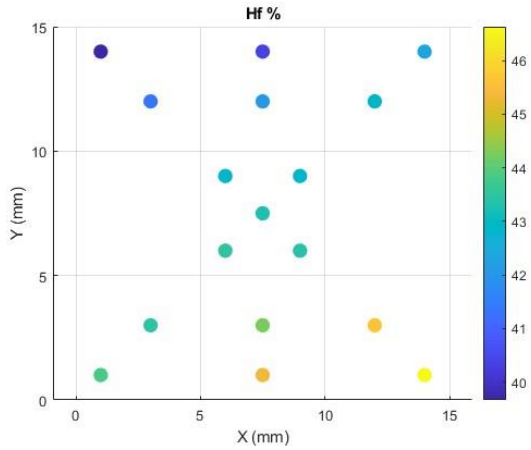

Figure B.4: chemical composition specimen HfTiAl

Bibliography

[1] M. Griffiths et al., “Effect of Neutron Irradiation on the Mechanical Properties of Austenitic Stainless Steels,” International Journal of Materials, 2021.

[2] Z. Dong et al., “Effects of Ion Irradiation and Temperature on Mechanical Properties,” Materials (o rivista analoga), 2023.

[3] Seinan Kogyo Co., Ltd., Company Website. Available: https://seinan-ind.co.jp/.

[4] S. O. Jeje, A. T. Alateeq, and S. S. R. K. Prasad, “Multi-Principal Element Alloy Coatings: A Review of Deposition Techniques, Applications and Future Prospects,” Metals and Materials International, 2025.

[5] M. P. Seah, "An accurate and simple universal sputtering yield function for elements, alloys and compounds," Nuclear Instruments and Methods in Physics Research Section B: Beam Interactions with Materials and Atoms.

[6] A. L. Barry et al., "Displacement damage in silicon due to electron irradiation: A review," IEEE Transactions on Nuclear Science.

[7] Kyoto Fusioneering, “The Necessity of Fusion Materials,” The Fusion Era, Dec. 11, 2023.

[8] D. B. Miracle and O. N. Senkov, "A critical review of high entropy alloys and related concepts," Acta Materialia,2017.

[9] R. A. Beale and A. C. Walker, "Corrosion resistance of hafnium and zirconium alloys in water-steam environments," Journal of Nuclear Materials, 1969.

[10] J.-W. Yeh, S.-K. Chen, S.-J. Lin, J.-Y. Gan, T.-S. Chin, T.-T. Shun, C.-H. Tsau, and S.-Y. Chang, "Nanostructured high-entropy alloys with multiple principal elements: Novel alloy design concepts and outcomes," Advanced Engineering Materials, vol. 6, no. 5, pp. 299-303, 2004.

[11] G. S. Was and D. Bei, "The use of high-entropy alloys for advanced nuclear applications," JOM, vol. 70, no. 6, pp. 872-879, 2018

[12] Y. Lu, C. T. Liu, M. Li, et al., “Irradiation resistance of Cantor high-entropy alloy”, Acta Materialia, 2013.

[13] F. Otto, et al., “The influences of temperature and microstructure on the corrosion of AlCrFeCoNi high-entropy alloys in simulated PWR environments”, Corrosion Science, vol. 149, 2019.

[14] Y. Ueda et al., "Roadmap for the development of fusion nuclear science and technology for DEMO and beyond," Nuclear Fusion, vol. 59, no. 9, 095001, 2019.

[15] D. M. Mattox, The Foundations of Vacuum Coating Technology. Springer Science & Business Media, 2003.

[16] R. F. Bunshah, Handbook of Deposition Technologies for Films and Coatings: Science, Applications and Technology. William Andrew, 1994.

[17] Richconn Technology Co., Ltd, "*Cos'è il rivestimento PVD? Una guida completa alla deposizione fisica da vapore*," **Richconn**, May 6, 2025. [Online]. Available: https://richconn.com/it/what-is-pvd-coating/. [Accessed: Nov. 7, 2025].

[18] H. O. Pierson, Handbook of Chemical Vapor Deposition: Principles, Technology and Applications, 2nd ed. Norwich, NY, USA: William Andrew Publishing, 1999.

[19] R. W. Johnson, A. Hultqvist, and S. F. Bent, "A brief review of atomic layer deposition: from fundamentals to applications," Materials Today, 2014.

[20] S. M. George, "Atomic layer deposition: an overview," Chemical Reviews, vol. 110, no. 1, pp. 111-131, 2010.

[21] JEOL Ltd., JSM-7001F Scanning Electron Microscope User's Manual, Tokyo, Japan, 2010.

[22] Keyence Corporation, VK-X 3000 Laser Microscope User's Manual, Osaka, Japan, 2020.

[23] Shimadzu Corporation, DUH-211/DUH-211S Instruction Manual, Shimadzu, Japan. [Online]. Available:

[24] J. Schneider, C. Hagendorf, S. Scholz, and H. M. Urbassek, "A simple model explaining the preferential (100) orientation of silicon thin films made by aluminum-induced layer exchange," Journal of Crystal Growth, vol. 287, no. 2, pp. 423–427, 2006.

[25] University of Tokyo, Exploration of radiation-resistant multicomponent solid-solution light alloys: Results report, Ministry of Education, Culture, Sports, Science and Technology (MEXT), Nuclear Systems R&D Project, Mar. 2025.